Bio-based aliphatic/aromatic poly(trimethylene furanoate/sebacate) random copolymers: Correlation between mechanical, gas barrier performances and compostability and copolymer composition

Bio-based aliphatic/aromatic poly(trimethylene furanoate/sebacate) random copolymers: correlation between mechanical, gas barrier performances and compostability and copolymer composition

Agata Zubkiewicz,[a] Anna Szymczyk,*[a] Rafaël J. Sablong,[b] Michelina Soccio,[c] Giulia Guidotti,[c] Valentina Siracusa[d] and Nadia Lotti *[c]

[a] Department of Mechanical Engineering and Mechatronics, West Pomeranian University of Technology, Al. Piastów 19, PL 70-310 Szczecin, Poland

[b] Polymer Technology Group/Eindhoven (PTG/e) B.V., De Lismortel 31, 5612 AR Eindhoven, The Netherlands

[c] Department of Civil, Chemical, Environmental, and Materials Engineering, University of Bologna, Via Terracini 28, 40131 Bologna, Italy

[d] Department of Chemical Science, University of Catania, Viale A. Doria 6, 95125 Catania, Italy

Correspondence author e-mail address: aszymczyk@zut.edu.pl, agata.zubkiewicz@zut.edu.pl, nadia.lotti@unibo.it

KEYWORDS: poly(trimethylene 2,5-furanoate), biobased copolyesters, barrier properties, mechanical properties, composability.

ABSTRACT. Highly promising fully biobased random copolyesters, poly(trimethylene 2,5-furandicarboxylate-*co*-trimethylene sebacate) (PTFcoPTSeb), were synthesized by using bio derived 1,3-propanediol, dimethyl ester of 2,5- furandicarboxylic acid, and sebacic acid, through eco-friendly polycondensation in the melt. Copolymers with high molecular weight containing 5,

15, 25 mol % of PTSeb were obtained, and their chemical structure confirmed by ^{1}H NMR and FTIR spectroscopy. The thermal, tensile and gas barrier properties and composability were studied in relation to the copolymer supramolecular structure. As expected, introduction of PTSeb co-units results in lowering of glass transition temperature of copolymers and improves their flexibility. Besides, all copolymers showed outstanding gas barrier properties to O_2 and CO_2, with copolymer containing 15 mol % of PTSeb showing exceptional gas barrier properties, better than those of PTF and comparable to those of EVOH, currently used in multilayer packaging films. The same copolymer exhibited temperature induced shape memory behaviour. It was found that low amounts (15-25 mol %) of PTSeb in copolymer significantly modifies PTF thermal, mechanical and barrier properties and renders the final material compostable. Copolyesters containing 15 and 25 mol % of PTSeb can compete in some applications with commercially available compostable Ecoflex® polymer, but with markedly improved barrier properties.

1. Introduction

Recently, furan based polyesters have been widely studied as new sustainable fully biobased alternatives to fossil or partially biobased polyesters such as poly(ethylene terephthalate) (PET) and poly(trimethylene terephthalate) (PTT), to cite two examples of thermoplastic polyesters, extensively used in packaging applications and more.[1][2][3] Among them, noteworthy is poly(trimethylene furanoate) (PTF) characterized by extraordinary barrier properties and interesting thermal and mechanical performances.[4][5] Its Young's modulus and glass transition temperature (T_g) are higher than those of PTT, whereas melting point is lower than PTT's one and much lower than that of PET (173 vs. 260 ºC).[1][6][7]PTF as PEF presents superior gas barrier properties than PET. PTF film permeability resulted indeed strongly reduced with respect to PET's one. For example, it possess 16-times lower O_2, 48-times lower CO_2, and 2 times lower water

permeability than PET film).[1][8] Thanks to these outstanding barrier performances, it will be possible to realize significantly lighter-weight packages. As known, their use can help reducing plastics volumes, thus lowering the carbon dioxide emissions during production and the costs related to shipping. Due to these smart performances, companies such as Du Pont and Archer Diels Midland (ADM)[9], and several other companies are interested in commercializing PTF, Avantium, on the other hand, being engaged in the commercialization of PEF.[10]

Furan based polyesters are developed not only for packaging applications, but also for the production of fibres,[11][12] and for engineering plastic applications. A recent study reports on PTF fibres, which exhibit lower crystallinity, higher hydrolytic degradation rate and are characterized by lower elastic modulus, lower tensile strength, but higher elongation at break compared to PTT ones.[12] Another recent work describes the results related to nanostructuring PTF film surface by using the technique of Laser Induced Periodic Surface Structures (LIPSS). It has been found that irradiation allowed the formation of periodic and nanometric ripples and no appreciable changes of macroscopic film properties after nanostructure formation occurred, differently from what previously found for the terephthalic counterparts, as PET and PTT. Even the surface mechanical properties of the nanostructured PTF were found to be improved, as evidenced by the increased Young's modulus for the nanostructured sample, opening the way to new possible niche areas of application for furan-based polyesters, such as organic electronics and medical devices, not concretely considered so far.[12][13]

On the other hand, PTF is not biodegradable or compostable, thus end-of-life options must be considered to avoid the accumulation of plastic waste. Like PET and PEF, PTF can be of course recycled, reducing carbon footprint, but in case of waste contamination with organic matter, compostability could represent the best option. Moreover, the applications of PTF can be limited

by its high rigidity and fragility, and slow melt crystallization rate. Therefore, recently, many researchers have applied copolymerization strategy to properly modify the properties of PTF and PEF by using a variety of aliphatic diacids and diols or cyclic monomers. [14][15][16][17][18] Blending with aliphatic or aromatic polyesters was also applied.[19][20][21] For example, PEF was copolymerized introducing ethylene sebacate co-units (ES) and thermal and mechanical properties appeared to be tunable with the copolymer composition.[22]

As is well known, a BASF product marketed under the trade name Ecoflex® has been on the market for more than 20 years.[23[24]Ecoflex is a random copolymer, composed by equal molar amount of aromatic (butylene terephthalate) and aliphatic (butylene adipate) comonomeric units and it can be considered an important example of partially aromatic biodegradable and compostable polymer based on fossil resources. Ecoflex is commonly used for the production of mulching foils for agriculture purposes, but it finds also application in the field of food packaging, thanks to its suitable mechanical and barrier properties to oxygen, carbon dioxide and water vapour.[23] Under composting conditions, its chemical structure allows a gradual biodegradation of the polymer, which takes approximately 3-4 months.

Therefore, the incorporation of aliphatic co-units along furan-based macromolecular chains appeared to be a good strategy to combine the typical biodegradability of aliphatic polyesters with the good thermal and mechanical properties of aromatic furan based polyesters. In fact, several examples of furan-based aromatic/aliphatic copolymers are reported in the literature. Random copolymers of PBF with glycolic acid or containing diglycolate moieties, characterized by superior thermal, tensile, barrier and degradation properties were proposed, as promising and innovative bio-based polymers for eco-friendly and sustainable plastic packaging by Hu and Soccio, respectively.[25][26]

Also, biobased poly(butylene succinate-*co*-furandicarboxylate) (PBSF) and poly(butylene adipate-*co*-furandicarboxylate) (PBAF) copolyesters were proposed as hydrolytic degradable polymers, with hydrolysis rate dependent on copolymer composition and crystallinity.[27][28] Such copolymers exhibit also sufficient good mechanical properties and are characterized by a good balance between hydrolytic degradability and durability.[27] It was also found that random copolyesters with higher BF content showed slower biodegradation, and PBAF degraded faster than PBSF at the same composition.[28]

As far as known, compostable packaging made from renewable biobased plant material as polylactic acid (PLA) and fossil based PBAT is still not yet a perfect solution. The copolymerization of PTF with sebacic acid could be one of the solutions if these copolymers will have desirable compostability.

In the present work, PTF was copolymerized with poly(trimethylene sebacate) (PTSeb) in order to improve its flexibility, overcoming all issues due to its high rigidity and fragility. Poly(trimethylene sebacate) (PTSeb) is a fully biobased castor oil and sugar derived biodegradable aliphatic polyester. It was therefore expected that the introduction of PTSeb co-units can also improve the biodegradability of the resulting material. The effect of the PTSeb co-unit content on the thermal, mechanical, gas barrier as well as compostability was studied. Lastly, but not least, we will show the aliphatic-aromatic copolymeric system object of the present paper could represent a credible biobased alternative to replace Ecoflex® in some applications.

2. Experimental section

2.1. Materials. Dimethyl-2,5-furandicarboxylate (FDCA-DME) (99.5 %) was delivered by Matrix Fine Chemicals GmbH (Switzerland). Sebacic acid dimethyl ester (SA-DME) (99 %) and tetrabutyl orthotitanate (TBT) (97 %) catalyst have been purchased from Sigma-Aldrich Co.

Pentaerythritoltetrakis[3-[3,5-di-tert-butyl-hydroxyphenyl]propionate (Irganox 1010) from BASF Corporation was used as antioxidant. Susterra® renewably sourced 1,3-propanediol (PDO) (98 %) was a gift from DuPont Tate & Lyle Bio Products Company, LLC (Loudon, TN, USA). PDO was purified by distillation before use and the other chemicals were used without any further purification.

2.2. Synthesis of PTFcoPTSeb copolymers. Poly(trimetylene 2,5-furanoate-*co*-trimethylene sebacate) (PTFcoPTSeb) copolymers syntheses have been carried out in the melt, starting from FDCA-DME, SA-DME, PDO and catalysts TBT, in a 1L stirred steel reactor (Autoclave Engineers Pennsylvania, USA) equipped with a condenser, a cold trap for collecting the by-products and a vacuum pump. First, predetermined amounts of FDCA-DME, SA-DME and PDO (see Table 1S in SI) in a molar ratio of diester/diol 1/2.2, were charged into the reactor and heated to 165 °C with continuous mechanical agitation under N_2 atmosphere. During the reaction, methanol as by-product was continuously removed from reaction mixture by distillation and collected in a graduate cylinder. When there was no methanol produced, the temperature was raised to 235 °C and the pressure reduced slowly during 45 min., and the polycondensation reactions was continued for 2.5-3 hours at a pressure of 15-20 Pa. Both steps, i.e. trans- esterification and polycondensation reaction were carried out in the presence of TBT catalyst (0.125 wt. % in each step in relation to diesters). Before the polycondensation step, the thermal stabilizer Irganox 1010 (0.5 wt. %) was introduced into the reaction mixture. The progress of the polycondensation reaction was monitored by observation of the change of the stirring torque in order to estimate the melt viscosity of the product at temperature of 235 °C. The process was stopped when the torque no longer increased. The molten polymer was extruded from the reactor into a water cooling bath, and then granulated and dried before processing. The neat PTF and PTSeb homopolymers were synthesized as

references under the same conditions. In the next step, the obtained materials were studied as received without any further purification.

2.3. Sample preparation. The injection moulded standard dumbbell shape specimens for tensile and DMTA tests were obtained by injection moulding using a Boy 15 injection moulding machine (Dr BOY GmbH&Co., Germany). The barrel temperatures were set to 190-200 °C, depending on the copolymer, while the mould temperature was 30 °C with a residence time in the mould of 15-30 s. The injection pressure and holding pressure were 75-90 MPa and 20-35 MPa, respectively, and the injection time was 6 s.

Films for testing barrier properties and composability were prepared by compression moulding using Collin P200E press, moulding polymers between Teflon films at temperatures of about 30 °C higher than their melting point. The pressure was progressively increased from 5 bar to 240 bar during 5 min, and the cooling time and cooling pressure were 45 s, and 120 bar, respectively. Films with thickness of about 100 μm and diameter of 11 cm have been prepared.

2.4. Characterization methods.

Proton nuclear magnetic resonance (^{1}H-NMR) spectroscopy analyses of samples dissolved in $CDCl_3$ (PTSeb, PTF25PTSeb samples) and in $CDCl_3$/CF_3COOD 10:1 (PTF5PTSeb, PTF15PTSeb samples) were performed using a Bruker spectrometer operating at 400 MHz. tetramethylsilane (TMS) was used as an internal chemical shift reference.

Fourier-transform infrared spectroscopy (FTIR) measurements were performed employing a Bruker Tensor-27 FTIR spectrophotometer in the range of 400 - 4000 cm^{-1} with a resolution of 2 cm^{-1}. Measurements were carried out using the attenuated total reflectance (ATR) technique.

Size exclusion chromatography (SEC) was used for the determination of the molecular weight distribution. Measurements were performed in 1,1,1,3,3,3-hexafluoro isopropanol (HFIP)

at 40 °C, on a system equipped with a Waters 1515 Isocratic HPLC pump, a Waters 2414 refractive index detector (35 °C), a Waters 2707 autosampler and a PSS PFG guard column followed by two PFG-linear-XL (7 μm, 8 × 300 mm) columns in series. HFIP with potassium trifluoroacetate (3 gL^{-1}) was used as the eluent at a flow rate of 0.8 mL min^{-1}. Calibration of the system was performed in relation to poly(methyl methacrylate) standards.

Thermogravimetric analyses (TGA) were carried out with a Setaram TGA 92-16 analyzer. Samples were heated in nitrogen or air atmosphere from 20 °C to 700 °C at a heating rate of 10 °C min^{-1}.

Differential scanning calorimetry (DSC) measurements were carried out on a Mettler Toledo DSC1 instrument. The instrument was calibrated with sapphires for the heat capacity and indium for the temperature. The glass transition, melting and crystallization of the samples were investigated in nitrogen atmosphere in the temperature range -60 - 200 °C, using aluminum pans to encapsulate the samples (ca. 10 mg). For applications, crystallization behavior of this materials is technical importance. Additionally, in order to study non-isothermal crystallization processes which can occur in the investigated samples during cooling and heating steps, the DSC scans where carried at scanning rates of 10, 5 , 3 °C/min. The degree of crystallinity (x_c) was calculated from the enthalpy of fusion, according to equation (1):

$$x_c = \frac{\Delta H_m - \Delta H_{cc}}{\Delta H_m^0} \cdot 100\% \qquad (1)$$

Where: ΔH_m is the heat of fusion estimated from the heating scan, ΔH_{cc} the correction due to heat of cold crystallization process, ΔH_m^0 the theoretical value of enthalpy for fully crystalline PTF (141.75 J g^{-1})[29] and for fully crystalline PTSeb (140 J g^{-1}).[30]

The shape memory properties (SMP) of PTF15PTSeb sample were monitored by means of cyclic thermo-mechanical analysis using a dynamic mechanical analyzer (DMA Q800, TA

Instruments), working in controlled strain mode. Polymer films of approximately 200 μm thick were tested. The measurements were performed following the procedure described in detail elsewhere.[31][32] Eight consecutive cycles consisting of heating – stress loading – cooling – stress unloading – heating were conducted. Programming of SMP was carried out at 50 °C (above T_g) and at 37 °C, while fixing of temporary shape was performed at 0 °C. Constant heating and cooling rate of 10 °C min^{-1} was maintained. The train fixity ratio (R_f) represents the ability to fix the mechanical deformation (ε_N) applied in the programming step; strain recovery ratio (R_r) represents the ability of the material to memorize/recover the permanent shape after the programming step. Both were quantified for each cycle with the following equations:

$$R_f(N) = \frac{\varepsilon_{N2} - \varepsilon_{N0}}{\varepsilon_{N1} - \varepsilon_{N0}} \times 100\% \qquad (2)$$

$$R_r(N) = \frac{\varepsilon_{N2} - \varepsilon_{(N+1)0}}{\varepsilon_{N2} - \varepsilon_{N0}} \times 100\% \qquad (3)$$

where: ε_{N0} – the initial strain for the Nth cycle , ε_{N1} – the maximum strain of stretched sample, ε_{N2} – the fixed strain after unloading, $\varepsilon_{(N+1)0}$ – the strain after recovering, also stands for the initial strain of the successive cycle. The average values and standard deviation for R_f and R_r were calculated based on three repeated measurements.

Tensile testing has been carried out by an Autograph AG-X plus universal testing machine (Shimadzu, Germany) equipped with a 1 kN Shimadzu load cell, a noncontact optical extensometer, and the TRAPEZIUM X computer software operating at a constant crosshead speed of 5 mm min^{-1}. Measurements were performed at room temperature on the dumbbell samples with a grip distance of 20 mm. According to PN-EN ISO 527 standard, Young's modulus, ultimate tensile strength (σ_u), strength at break (σ_b) and elongation at break (ε_b) of PTF and copolyesters were determined. The reported values are the mean values of seven measurements.

X-ray diffraction (XRD) measurements were performed on amorphous and annealed injection molded samples and films over the 2θ range from 4 to 60°, at steps of 0.02° using a X'Pert PRO PANalytical diffractometer operating with Cu Ka radiation (λ = 0.154 nm), at 40 kV and 30 mA. The indexes of crystallinity (x_c) were evaluated from the XRD profiles by the ratio between the crystalline diffraction area (A_c) and the total area of the diffraction profile (A_t), $x_c = A_c/A_t$. The crystalline diffraction area has been obtained from the total area by subtracting the amorphous halo.

Permeability tests to dry O_2 and CO_2 were performed at 23 °C by using a manometric method with a Permeance Testing Device, GDP-C (Brugger Feinmechanik GmbH), according to ASTM 1434-82 (standard test method for determining gas permeability characteristics of plastic film and sheeting, 2009), DIN 53 536 (gas permeability determination) in compliance with ISO/DIS 15105-1 (Plastic film and sheeting determination of gas transport rate: - Part I: Differential pressure method, 2007) and according to Gas Permeability Testing Manual (Registergericht München HRB 77020, Brugger Feinmechanik). The instrument is composed by two chambers, in between the polymeric film (sample area of 11.34 cm^2) is placed, the upper one being filled with the test gas (1 atm, gas stream of 100 cm^3 min^{-1}), the lower one containing a pressure transducer. The sample temperature was set by an external thermostat HAAKE-Circulator DC10-K15 type (Thermoscientific, Selangur Darul Ehnsan, Malaysia). By measuring gas pressure as a function of time and volume of the device, permeability values (gas transmission rate, GTR) through polymeric films were calculated by the software. The obtained GTR values were normalized for the film thickness, and reported as average of three measurements.

Compostability tests on a lab scale were performed in order to evaluate how the copolymerization carried out in this study affects PTF compostability. To this aim, weight loss

measurements and DSC analysis of partially degraded samples were performed. More in detail, these tests were carried out at 58 °C and relative humidity of 99 %, using mature compost kindly supplied by HerAmbiente S.p.A. Prior to degradation experiment, squared samples of each polyester (15 x 15 mm) were immersed in a 70 % ethanol solution, washed repeatedly with deionized water, and stored at room temperature to constant weight. These samples were weighed and then immersed between two layers of wet compost. At different timepoints, duplicates of each sample were collected from compost, washed repeatedly in a 70 % ethanol solution under stirring (to remove residual compost adhered on the films), washed again with deionized water, and dried at room temperature to constant weight. Lastly, residual gravimetric weight was measured.

Morphological investigations of gold sputter-coated partially degraded samples were performed by means of a Hitachi S-2400 scanning electron microscope, operating at 15 kV.

3. RESULTS AND DISSCUSION

3.1. Structure and composition of PTF-PTSeb copolymers.

A series of novel fully biobased PTFcoPTSeb copolymers with aliphatic co-unit content ranging from 5 to 25 mol % were successfully synthesized by melt polycondensation. The chemical structure of the synthesized copolymers is presented in Figure 1 and their composition and molecular weight are collected in Table 1. The chemical structure of the synthesized copolyesters was confirmed by FTIR and ^{1}H-NMR analysis. The FTIR spectra of the PTF and PTFcoPTSeb copolymers are shown in Figure 2.

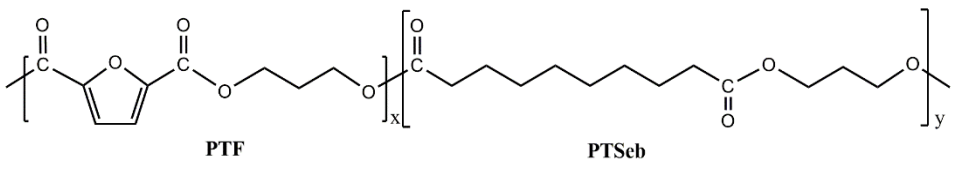

Figure 1. Chemical structure of PTFcoPTSeb copolymers.

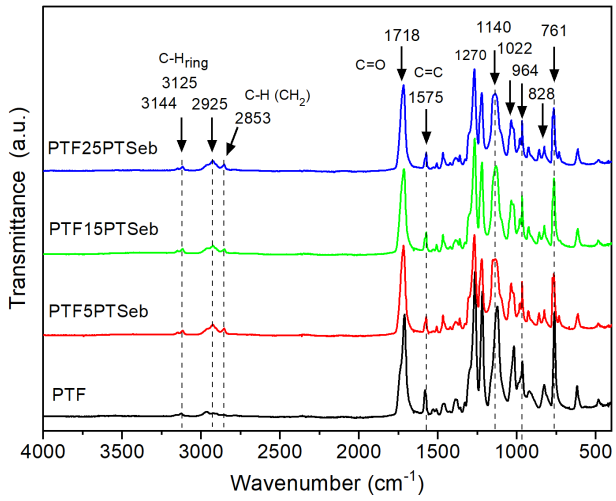

Figure 2. FTIR spectra of PTF and PTF-PTSeb random copolymers.

The spectra showed indeed typical vibration modes of furan based polyesters.[33] The peak at 1718 cm^{-1} indicated the stretching vibration of the carbonyl group (C=O) in the ester, and the stretching vibration peak of the bond C-O-C was shown in the signal at 1140 cm^{-1}. These two peaks confirmed the presence of ester bonds in the synthesized copolyesters. In addition, in all samples, the characteristic transmittance peaks of the furan ring were observed. In detail, we can see the weak symmetrical and asymmetrical C-H stretching vibrations of C-H at 3144 and 3125 cm^{-1}, C=C at 1575 cm^{-1}, the furan ring breathing vibration at 1022 cm^{-1} and ring bending vibration at 964, 826 and 761 cm^{-1}. Two weak bands near 2925 and 2853 cm^{-1} due to the symmetrical and asymmetrical C–H stretching characteristics of the -CH_2- groups of the propylene glycol, corresponding to the ester bond and sebacate unit are also present. The intensity of these bands increased with the molar content of PTSeb units in copolyesters. Moreover, the strong signal assigned to =C-O-C= antisymmetric stretching and =C-O-C= ring vibrations appears at 1265-1269 cm^{-1}, and 1218-1223

cm^{-1} accordingly. As expected, the intensities of these peaks characteristic of furan ring decreased as the amount of PTSeb in the copolymers increased.

The copolymer chemical structure was also verified through ^{1}H-NMR spectroscopy (Figure 3) which, in addition, permitted to estimate the effective copolymer composition, to calculate the sequence length and their distribution along the macromolecular chain.

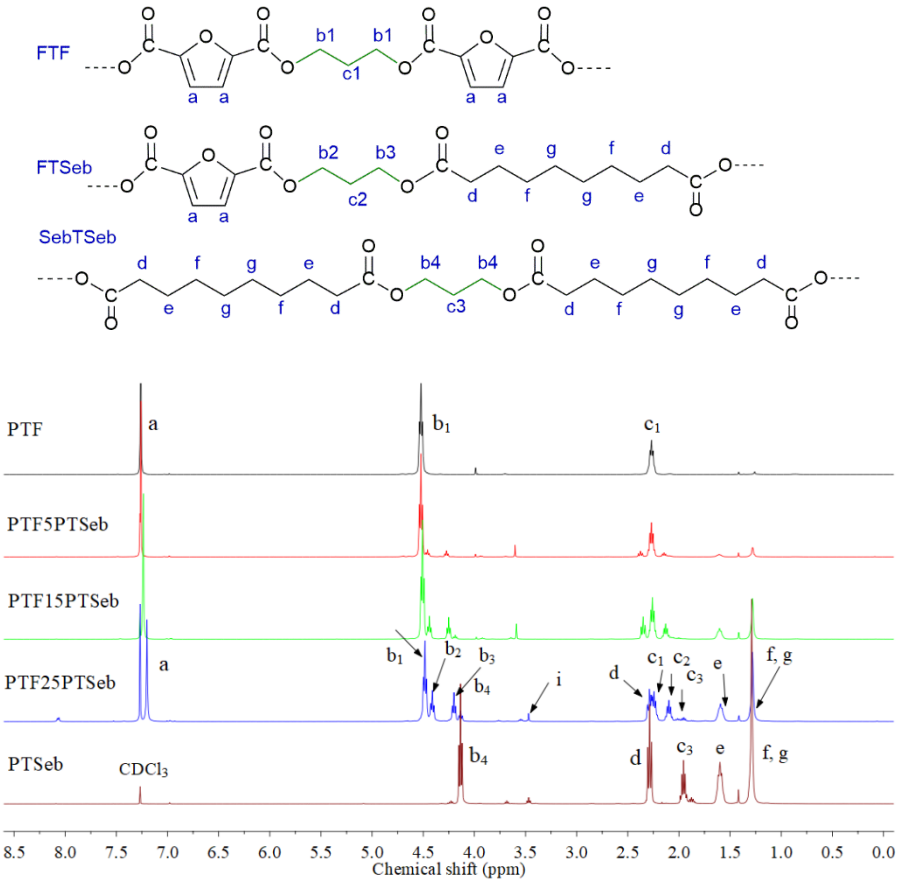

Figure 3. ^{1}H-NMR spectra of PTSeb, PTF25PTSeb in $CDCl_3$ and PTF, PTF5PTSeb, PTF15PTSeb in $CDCl_3$/CF_3COOD 10:1 with relative peak assignment.

In Figure 3, for the sake of comparison, the spectrum of PTSeb homopolymer is also presented. The PTSeb spectrum showed peaks corresponding to the CH_2 groups of the sebacate unit at 2.29

(4H, m, peak d), 1.60 (4H, m, peak e), and 1.29 (8H, m, peaks: f, g) ppm, and to CH_2 groups of the propylene unit at 4.13 (4H, m, b_4) and 1.87 (2H, m, c_3) ppm. The signal at 2.29 ppm corresponds to the CH_2 protons in aliphatic units of the sebacate connected to ester bond (-CH_2-C(O)O-, peak d). A very small peak from protons in methylene end group in PDO at 3.47 ppm (t, CH_2-OH,) is observed as well.

In the PTF spectrum, the peak at 7.26 ppm (2H, s, CH, a) was attributed to protons in the furan ring and the peaks from the three methylene groups of the oxypropylene units appear at 4.52 (4H, m, -C(O)-OCH_2-, peak b_1) and 2.27 ppm (2H, m, CH_2, peak c1). The protons from the methylene groups in oxypropylene unit next to C(O)O group in the furanoate and sebacate units give peaks at 4.41 (2H, m, CH_2, b_2) and 4.20 ppm (2H, m, CH_2, b_3), respectively, and the other methylene group originates peak at 1.89 ppm (2H, m, CH_2, c_2).

The integration of proton resonance intensities for the characteristic signals b_4, b_3, b_2 and b_1 from the TSeb and TF units were employed to calculate (eq. 1) the corresponding molar fraction of PTSeb in copolymers. The degree of randomness (R) of the synthesized copolyesters was calculated from the equation (2), where $L_{n,TF}$and $L_{n,TSeb}$ represent the number-average sequence length (eq. 3 and 4) of trimethylene furanoate (TF) and trimethylene sebacate (TSeb) units, respectively.

$$x_{PTSeb}\,(mol\,\%) = \frac{I_{b3}+I_{b4}}{I_{b1}+I_{b2}+I_{b3}+I_{b4}}\,x\;100\;\% \qquad (1)$$

$$R = {}^{1}/_{L_{n,TF}} + {}^{1}/_{L_{n,TSeb}} \qquad (2)$$

$$L_{n,TF} = 1 + I_{c1}/I_{c2} \qquad (3)$$

$$L_{n,TSeb} = 1 + I_{c3}/I_{c2} \qquad (4)$$

where: I_{b1}, I_{b2}, I_{b3}, I_{b4}, I_{c1}, I_{c2}, I_{c3} represent the integrals of the corresponding peaks (Figure 3).

The calculated values of mol % of PTSeb units in copolymers presented in Table 1 are close to the corresponding feed molar ratio. As seen in Table 1, the degree of randomness was close to 1, indicating the random nature of the copolyesters under investigation. All polyesters presented high number average molecular weights (M_n) in the range 34 000 - 51 000 g/mol and polydispersity indexes (PDI) typical for polycondensation processes (i.e. ≥ 2) (see Table 1). It can be assessed that, in all cases, molecular weights reached the plateau value.

Table 1. Composition, sequence length, degree of randomness and molecular weight of the PTFcoPTSeb copolymers.

Sample	In the feed	^{1}H-NMR				Mn	Mw	PDI
	φ_{PTSeb} (mol %)	φ_{PTSeb} (mol %)	$L_{n,TF}$ -	$L_{n,TSeb}$ -	R -	(g mol^{-1})	(g mol^{-1})	
PTF	0	0	-	-	-	34 460	69 610	2.02
PTF5PTSeb	5	5.26	8.692	1.154	0.98	42 810	100 630	2.35
PTF15PTSeb	15	14.39	4.030	1.182	1.09	43 040	105 160	2.44
PTF25PTSeb	25	24.48	2.473	1.421	1.10	51 010	139 100	2.72
PTSeb	100	-	-	-	-	22 280	45 450	2.04

3.2. Thermal transitions and degree of crystallinity of PTFcoPTSeb copolymers

The phase behaviour and the supramolecular structure of PTF and PTFcoPTSeb copolymers were evaluated by DSC and XRD. In particular, the thermal behavior of injection molded samples has been investigated before and after annealing treatment. In our earlier study, we reported PTF is characterized by a low crystallization ability.[4] Whence, in order to establish the effect of the presence of TSeb co-units on PTF non-isothermal crystallization process which can occur during the heating and cooling steps, further DSC scans were carried out at different scanning rates. The corresponding DSC heating and cooling curves at different rates are shown in Figure 4. Lastly, the

thermal behavior of compression molded films, strictly correlated to gas barrier response and to compostability, has been also analyzed. All the thermal results are collected in Table 2, together with those of some PBAT copolymers,[23][34] and Ecoflex®,[35][36] which were added for sake of comparison.

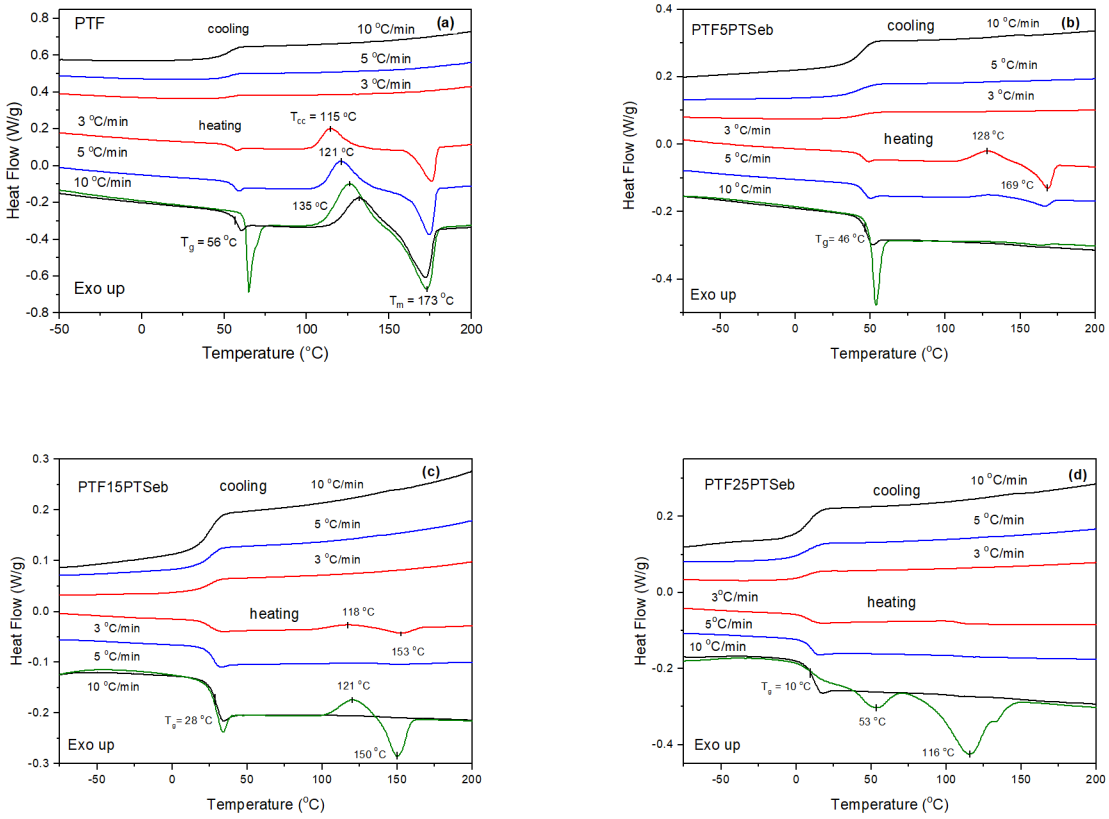

Figure 4. DSC heating and cooling scans at rate of 10, 5 and 3 °C min^{-1} for PTF (a) and PTFcoPTSeb copolymers (b-d). For all samples, the first heating scan measured at 10 °C min^{-1} after 2 month storage at room temperature are reported (green curves).

Table 2. DSC data from first scans at 10 °C min^{-1} for PTF and PTFcoPTSeb copolymers, together with those of some PBAT copolymers and Ecoflex.

Sample	T_g (ºC)	ΔC_p (Jg^{-1}°C^{-1})	T_{cc} (°C)	ΔH_{cc} (Jg^{-1})	T_{m1}, T_{m2} (°C)	ΔH_{m1}, ΔH_{m2} (Jg^{-1})	x_c (%)	x_c (XRD) (%)
PTF	62	0.39	126	29.05	173	30.54	1.05	-
PTF an100/1h*[a]	56	0.27	-	-	174	34.0	24.00	20.3
PTF film	64	0.35	129	30.76	173	30.77	-	-
PTF5PTSeb	46	0.42	-	-	-	-	-	-
PTF5PTSeb an100/1h*[a]	45	0.11	-	-	105, 167	2.16, 35.7	26.70	27.3
PTF5PTSeb film	50	0.33	130	2.64	165	3.25	0.43	-
PTF15PTSeb	28	0.46	120	4.30	150	5.18	0.62	-
PTF15PTSeb an50/24h*[b]	28	0.43	120	5.01	150	12.50	5.29	7.0
PTF15PTSeb an80/1h*[c]	30	0.30	-	-	87, 148	3.32, 34.94	26.99	25.1
PTF15PTSeb film	25	0.35	99	24.36	150	28.17	2.7	-
PTF25PTSeb	10	0.27	-	-	53, 116	5.31, 26.87	22.70	18.6
PTF25PTSeb an50/24h*[b]	10	0.13	-	-	69, 117	5.05, 25.99	21.89	20.4
PTF25PTSeb film	7	0.20	-	-	60, 117	7.09, 25.75	23.16	-
PTSeb	-50	0.23	-	-	54	65.79	46.99	-
PBAT with 48 mol % of BA[d] [34]	-25	-	-	-	56, 137	3.8, 18.2	22.7	-
PBAT with 57 mol % of BA[e] [23]	-33	-	-	-	128	9.5	8.3	-
Ecoflex® F-Blend C1200[f] BASF [35][36]	-30	-	-	-	121	22.2	19.5	-
	-31	-	-	-	126	18	15.9	-
Eastar Bio Ultra Copolyester 14766,[g] EASTMAN [37]	-38	-	-	-	110	12.3	10.8	-

*[a] annealed at 100 ºC for 1h; *b - annealed at 50 ºC for 24 h; *c - annealed at 80 ºC for 1 h;

[d] synthesized PBAT copolymer containing of 48 mol % of BA with R = 1.02 and M_w = 93 000 g/mol, PDI = 2.06;[34]

[e] synthesized PBAT copolymer containing of 57 mol % of BA with R= 1.02;[23]

[f] PBAT containing 51 mol % of BA, R= 0.998, and M_w = 76 200 g/mol, PDI = 1.89; [36]

[g] PBAT containing 57 mol % of BA with M_w= 48 000 g/mol, PDI = 2.4, d = 1.27 g cm^{-3}.[37]

PTSeb homopolymer has glass transition temperature (T_g) at -50 ºC and melting point (T_m) at 54 ºC (Figure 1S) indicating that at room temperature (T_{room}) it is a semicrystalline polyester with a

highly mobile amorphous phase. On the contrary, at T_{room}, PTF is an amorphous polymer, having T_g at 62-64 ºC. As seen in Figure 4a, PTF is able to crystallize during heating once T_g is exceeded, but in comparison to its well known terephthalic counterpart PTT, its rate of crystallization is significantly lower. In addition, being the crystallization enthalpy comparable to the melting one, it can be assessed that PTF is a completely amorphous material. During the cooling from the melt at rates 3, 5 and 10 ºC min^{-1}, no crystallization exotherm was indeed observed.

Also, PTFcoPTSeb copolymers do not undergo any crystallization during cooling from the melt. Furthermore, for PTF, at the heating rate of 10 ºC min^{-1}, we can observe a cold crystallization exotherm at 135 ºC (82 ºC above T_g) followed immediately afterward by a melting endotherm with a peak maximum at 173 ºC. At heating rate of 3 ºC min^{-1}, the peak of cold crystallization is shifted to lower temperature (115 ºC). PTF annealed at 100 ºC for 1 hour develops a crystallinity of 24 % (Table 2).

The copolyesters did not show any cold crystallization peak at heating rate of 10 ºC min^{-1} (Figure 4b-d). However, at lower heating rates, their ability to crystallize during heating decreased with increasing PTSeb unit content. For PTF15PTSeb, at heating rate of 3 ºC min^{-1}, an exotherm followed by an endotherm, both of small intensity, were present at 118 ºC (ΔH_{cc}= 3.4 J g^{-1}) and at 153 ºC (ΔH_m= 3.5 J g^{-1}), respectively. In case of PTF25PTSeb, the crystallization process could not be detected during neither DSC cooling, nor heating process, when heating/cooling rates were 10, 5 and 3 ºC min^{-1}. That indicates the crystallizing ability of this copolymer is strongly reduced.

Anyway, in case of PTF25PTSeb, the DSC profile changed significantly after storage at room temperature for several days and months. Indeed, as can be seen in Figure 3S, a crystalline structure was developed after for 4 days storage at room temperature. After T_g, a multiple endothermic phenomenon is evident, consisting of a main peak located at about 114 -116 °C with a quite well

defined shoulder on the high temperature side and a smaller peak at 45-70 °C. Besides, the first small endotherm moves to higher temperature with increasing storing time at room temperature. The presence of two separated endotherms could be related to the polymorphism, which characterizes PTF. For PTF homopolymer, the shift of the small endotherm to higher temperature was observed with the increasing of crystallization temperature.[38] The degree of crystallinity estimated through DSC was around 22 %, for annealed PTF25PTSeb sample. This result was expected in some way, if we consider this copolymer is characterized by a glass transition temperature below room temperature, meaning that the amorphous macromolecular chains are in a mobile state and can rearrange and crystallize.

As to the glass- to-rubber-transition, the introduction of flexible aliphatic TSeb units determined a decrease of T_g from 46 to 28 and 10 ºC for PTF5PTSeb, PTF15PTSeb, and PTF25PTSe, respectively. The unique T_g was in accordance with the random structure determined by ^{1}H-NMR. The T_m also decreased with increment of TSeb unit content in copolyesters, as typically happens in statistical copolymers with both co-units able to crystallize, but only the one present in larger quantity taking part in the crystallization process. The low crystallizing ability of PTF both from the melt and the glassy state compared to PTT can be correlated to asymmetrical polymer chemical structure because of furan rings. The higher T_g can be instead associated to higher interchain interactions, due to polar character of furan ring.[39]Introduction of TSeb units do not accelerate crystallization ability of copolyesters. Therefore, it can be established that PTF and PTFcoPTSEb copolyesters containing 5 and 15 mol % of PTSeb co-units are amorphous polymers, the first two containing a glassy amorphous phase, the last containing a semi-mobile amorphous phase at room temperature.

As already mentioned, the copolymer with the highest content of trimethylene sebacate units is able to evolve over time, being characterized by a T_g below room temperature. In fact, after 4 days at 23 ° C, it develops a consistent crystalline phase and therefore has a different phase behavior compared to the other samples under study (semi-crystalline with a mobile amorphous phase). In order to explore the microstructure of all the polymers under study, XRD measurements have been carried out before and after annealing treatment. The corresponding XRD profiles are shown in Figures 5 and 5S.

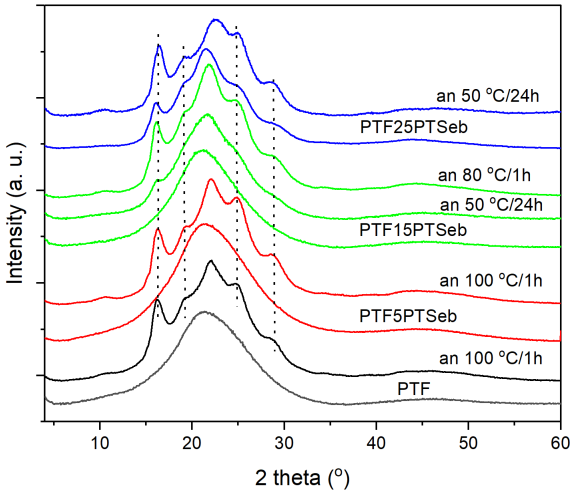

Figure 5. Comparative XRD patterns for PTF and PTFcoPTSeb copolymers before and after annealing.

Before annealing, the patterns of all samples with the exception of PTF25PTSeb are typical of amorphous polymers. In fact, the diffraction profiles did not show any diffraction peaks, but rather the amorphous halo at 2θ = 21 °C, in accordance with calorimetric results. After annealing at 100 °C for 1 hr, PTF XRD profile showed diffraction peaks located at values of 2θ: 16.22, 18.97, 22.03, 25.03 and 28.83° (corresponding to d = 5.46, 4.69, 4.03, 3.44, 3.09 Å). All the reflections are broad and characterized by low intensity, indicating the developed crystalline structure is imperfect. As

recently reported by Righetti and co-workers,[38][40] PTF exhibits polymorphism: three forms (named α, α' and β) have been identified, depending on the crystallization temperature. These different crystal modifications can also coexist, and crystal transformation from a less to a more perfect crystal structure can occur upon heating. According to Righetti et al.'s[38] results, annealed PTF sample object of the present study developed α' phase, a looser and disordered crystal structure. In the semicrystalline copolymers, we can observe all the characteristic peaks of PTF, indicating the crystalline phase present is PTF one; peak position keeps constant (see dashed line in Figure 5, added as guide for the eyes) with the exception of the large reflection located at 2θ =22°, which in all the copolymers moves to lower angles (i.e. longer d spacings), except for annealed PTF25PTSeb. In this last case, compared to PTF homopolymer, the reflection indeed shifted towards larger angles. Righetti in her work pointed out α and α' forms are very similar, the α modification being characterized by a more perfect structure (the corresponding characteristic reflection is indeed located at slightly higher angle, 2θ = 23°). It is also worth remembering that by copolymerization it is possible to selectively favor the formation of a different crystal form with respect to the one present in the parent polymorph homopolymer.[41] It is thus plausible that in the annealed copolymer with the highest amount of aliphatic co-units, the formation of the more perfect α phase also occurs, with α' and α forms coexisting, this latter being favored with respect to α' one. Further studies to shed light on these results are ongoing and will be published in a future paper.

Annealing treatment determined the development of a crystalline phase in PTF and in PTF5PTSeb, although the copolymer crystalline fraction was slightly lower. No appreciable effect was observed for PTF15PTSeb, whereas for the copolymer richest in aliphatic co-units, the sample stored at 25 °C for 2 months and the one annealed at 50 °C for 24 hours were characterized by the

same fraction of crystal phase. As far as PTF15PTSeb copolymer is concerned, annealing treatment did not appreciably favors the development of a crystal phase because the annealing temperature (50 °C) was just above its glass transition temperature, and thus the macromolecular chains did not acquire enough mobility to rearrange and crystallize. Anyway, by increasing annealing temperature (80 °C), after only 1 hour of thermal treatment the development of some slight reflections located at the same position of PTF ones can be observed, indicating that at this temperature polymeric chains have enough energy to crystallize.

By comparing the thermal transitions of the copolymers under investigation with biodegradable fossil-based PBAT,[23][34] it is possible to notice how T_g of this latter is well below room temperature, amounted to about -30 °C, whereas T_m values are almost comparable to T_m of PTF25PTSeb (see Table 2). In addition, ΔH_m and x_c values range from 9.5 to 22.2 J/g and from 8.3 to 22.7 %,respectively. More specifically, the commercially available PBAT copolymers (Ecoflex® - BASF, Germany; Estar Bio® - EASTMAN, USA), (with molecular weight ranging from 48 000 to 93 000 g/mol), have a T_m of 110 -126 °C, and T_g of -30 to -38 °C and can crystallize at 67-100 °C during cooling from the melt.[36][42][43] In conclusion, in comparison to them, PTFcoPTSeb copolymers are characterized by higher values of T_g and T_m, but their rate of crystallization is much slower than PBAT.

3.3. Thermal stability

In order to evaluate the thermal stability of the synthesized copolyesters, their thermal degradation behavior under both oxidative (air) and inert (argon) atmosphere were studied by TGA (Figure 4S). Thermal stability was evaluated by determining the temperature of 5 % weight loss ($T_{d5\%}$),the temperature at which the maximum decomposition rate was observed (T_{DGTmax}) and the

residual weight at 600 ºC (R). All data are summarized in Table 3, together with those of PBAT in inert atmosphere, reported for sake of comparison.[23]

Table 3. TGA data for PTF and PTFcoPTSeb copolymers in air and inert atmosphere.

Sample	Oxidative atmosphere			Inert atmosphere		
	$T_{d5\%}$ (ºC)	T_{DTGmax} (ºC)	R (%)	$T_{d5\%}$ (ºC)	T_{DTGmax} (ºC)	R (%)
PTF	364	390	1.9	356	388	1.1
PTF5PTSeb	364	391	1.5	365	395	5.4
PTF15PTSeb	360	394	0.7	365	395	6.7
PTF25PTSeb	365	400	0.6	366	397	6.3
PTSeb	362	406	0.9	365	418	4.6
PBAT with 57 mol % BA[A][23]	-	-	-	351	390	5.0
Ecoflex® BASF [B][43]	357	400	-	358	401	-

$T_{d5\%}$ - temperature corresponding to 5 % weight loss; T_{DTGmax} - temperature at maximum of weight loss rate; R – residue at 600 ºC; A - PBAT copolymer containing of 57 mol % of BA, B- PBAT copolymer containing of 56 mol % of BA and Mw=140 kDa supplied by BASF.[43]

It was noticed that PTF and PTSeb present a relatively high thermal stability in both oxidative and inert atmospheres. Like for PTF, all copolyesters, in both atmospheres, are characterized by a $T_{d,5\%}$ in the temperature range 356 - 366 ºC (Table 3), and by a T_{DGTmax} in temperature range of 388 - 400 ºC. This indicates that all copolymers are thermally stable during processing conditions. For copolymers, $T_{DGT,max}$ is slightly shifted (1-10 ºC) to higher temperatures in comparison to PTF. This is probably caused by the presence of longer aliphatic chains present in TSeb co-unit: indeed, our and recent studies on thermal stability of PTSeb indicate that this polyester is thermally stable and has high decomposition rate (413-418 ºC). Degradation mechanisms of the PTSeb and PTF homopolymers are presented in more detail in refs[44][45] From the analysis of the $T_{d5\%}$ in inert

atmosphere, it is noticeable that PTFcoPTSEb copolymers are all more thermally stable than PBAT. The same result can be observed also for T_{DTGmax}, with the only exception of PTF. R values progressively increase with the amount of TSeb co-units, ranging from 1.1 to 6.3 % in inert atmosphere, whereas in oxidative atmosphere an opposite trend can be observed, being however in all cases lower than 2%.

3.4. Tensile properties and shape memory behaviour of PTFco15PTSeb copolymer

Tensile tests were performed subjecting the samples to a constant deformation speed, by measuring the stress variation as a function of the elongation. Figure 6 shows representative stress-strain curves of PTF and PTFcoPTSeb copolymers before and after annealing.

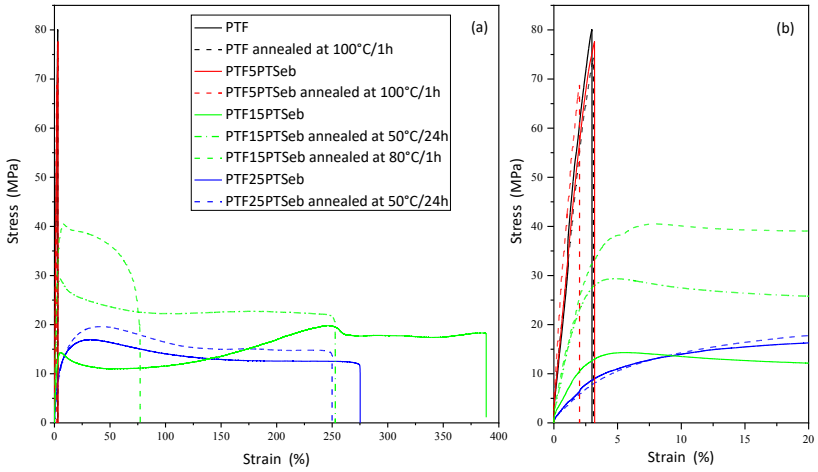

Figure 6. Stress-strain curves for PTF and PTFcoPTSeb copolymers before and after annealing (a) magnification of the region corresponding to small strain range (0-20%) (b).

The tensile stress, stress at break and elongation at break were determined and summarized in Table 4. In the same Table, mechanical data of some PBAT copolymers and Ecoflex are also reported for comparison purposes. As expected, by increasing the content of PTSeb units above 5 mol %, Young's modulus and tensile strength decrease, in agreement with the decreasing of T_g observed by DSC analysis.

Table 4. Tensile properties of PTF and PTFcoPTSeb copolymers before and after annealing, together with those of some PBAT copolymers and Ecoflex.

Sample	Young's modulus (MPa)	Ultimate tensile stress (MPa)	Stress at break (MPa)	Elongation at at break (%)
PTF	2460 ± 376	79 ± 3	79 ± 3	3 ± 1
PTF an100oC/1h	2707 ± 164	73 ± 1	73 ± 1	3 ± 1
PTF5PTSeb	2534 ± 175	77 ± 1	77 ± 1	3 ± 1
PTF5PTSeb an100°C/1h	3705± 322	69 ± 2	69 ± 2	3 ± 1
PTF15PTSeb	574 ± 79	17 ± 1	17 ± 1	410 ± 20
PTF15PTSeb an 50°C/1h	1277 ± 104	30 ± 2	23 ± 1	240 ± 60
PTF15PTSeb an 80°C/1h	1481 ± 229	42 ± 2	19 ± 1	73 ± 11
PTF25PTSeb	289 ± 63	17 ± 1	12 ± 1	250 ± 35
PPTF25PTSeb an 50°C/24h	414 ± 8	18 ± 1	13 ± 1	215 ± 33
PBAT with 57 mol % of BA[a] [23]	87 ± 8	30 ± 1	30 ± 1	870 ± 44
PBAT with 59 mol % of BA[b] [46]	76 ± 4	6 ± 1	6 ± 1	122 ± 23
Ecoflex® F blend C1220,[c] BASF[35]	81 ± 2	20 ÷ 2	20 ÷ 2	689 ± 110
Ecoflex® F bland C12000,[d] BASF[36]	120 ± 2	19 ± 1	19 ± 1	575 ± 2

a – measured for synthesized PBAT, on specimens obtained by hot pressing the polymers and then cut with a standard cutter to dumbbell-shaped specimens and at a crosshead speed of 50 mm min^{-1};[23]
b – measured for synthesized PBAT with M_w = 45 000 g/mol (PDI =1.6) at a crosshead speed of 50 mm min^{-1};[46]
c - measured for PBAT with M_w = 53 900 g/mol (PDI = 1.70) on dog-bone specimens cut from compressed sheds tests for 1 mm film thick, at stretching rate of 5 mm min^{-1};[35]
d - measured for PBAT with 52 mol % of BA with Mw = 76 000 g/mol (PDI = 1.89) on dog-bone specimens cut from compressed sheds tests for 1 mm film thick, at a crosshead speed of 5 mm min^{-1}.[36]

As to strain at break, PTF and PTF5PTSeb copolymer were the most brittle materials among the family, being characterized by a small elongation at break, not exceeding 3 %. It must be reminded that both the samples are in their glassy state at room temperature. For samples with T_g around or below room temperature, the mechanical behaviour changes significantly. By increasing the

amount of the PTSeb co-units, the copolymers became more ductile and their elongation at break exceeded 240 %, PTF15PTSeb copolymer reaching even a value of 410 %, thanks to the higher flexibility conferred by PTSeb co-units. Furthermore, it has to be emphasized for PTF25PTSeb copolymer, the DSC glass transition temperature was lower than temperature at which the samples were tested ($T_{test} = T_{room}$).

The value of Young's modulus for PTF25PTSeb copolymer was therefore relatively low and did not exceed 300 MPa. Moreover, for PTF15PTSeb copolymer, strain hardening effect can be observed after 6 % of elongation. Interestingly, the strain at break of this sample is much higher than that of PTF25PTSeb, although T_g of the latter copolymer is lower. This result can be ascribed to the high crystallinity degree of the copolymer richer in PTSeb units, thus reducing polymer flexibility.

The same experiments were carried out on the samples subjected to annealing. After this treatment, the materials became less ductile and their elongation at break decreased, due to the crystallinity developed in the samples, according to XRD results (Figure 5, Table 2). The increase in the degree of crystallinity contributed also to a slight increase in tensile strength. Copolymers annealed at temperature of 50 ºC above T_g show a significant increase of Young's modulus.

Compared to other PBAT23,[46] and very ductile Ecoflex®,[35][36][43] characterized by a low elastic modulus (< 100 MPa) and a very high elongation at break , the obtained PTFcoPTSeb copolymers showed higher values of Young's modulus, while Ecoflex strain at break is intermediate between those of PTF5PTSeb and PTF15PTSeb. PTF15PTSeb copolymer appeared to be the sample with the mechanical performance more similar to PBAT (Table 4), even though characterized by a higher modulus and lower stress and elongation at break. However, it must be

specified that Ecoflex contains higher amount of aliphatic comonomeric units (around 50 mol %).[36][47]

In addition, it was found that the copolymer containing 15 mol % of PTSeb with T_g of 28 °C behaves as temperature induced shape memory polymer (SMP). The shape memory effect is presented in Figure 7; a dumbbell shape PTF15PTSeb copolymer sample was heated to 50 ºC and then bent. By cooling, the shape was fixed. After reheating, the sample began to return to its original dumbbell shape, reaching it after 3 minutes.

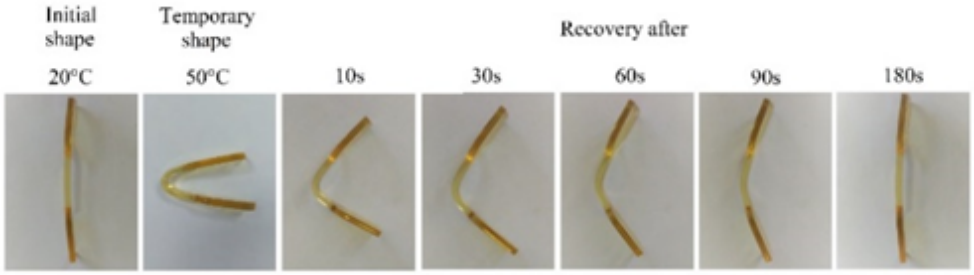

Figure 7. Demonstration of shape recovery of dumbbell shape sample of PTF15PTSeb copolymer.

It is known that the shape storage and recovery occur through a temperature-dependent conversion of the flexible/rubbery phase to the glassy one during cooling and conversely during heating. In semicrystalline polymers, shape storage and recovery can occur either through the glass transition of the amorphous region or the melting of the crystalline region. When amorphous polymer is at temperature above T_g, the chains are mobile and respond instantly to an applied load, to minimize the configurational entropy.[48] Besides, in amorphous polymers an exponential change in the mobility of the polymer chains with temperature is observed. The mobility decreases with temperature and the polymer mechanical behavior becomes increasingly slow.

In order to investigate the shape memory properties of the PTF15PTSeb copolymer in more detail, DMTA cyclic analysis was performed. The sample was heated above T_g (50 °C was used as

deformation temperature), stretched and then cooled down. Figure 8A presents shape memory cycles, with 50 °C as the deformation temperature.

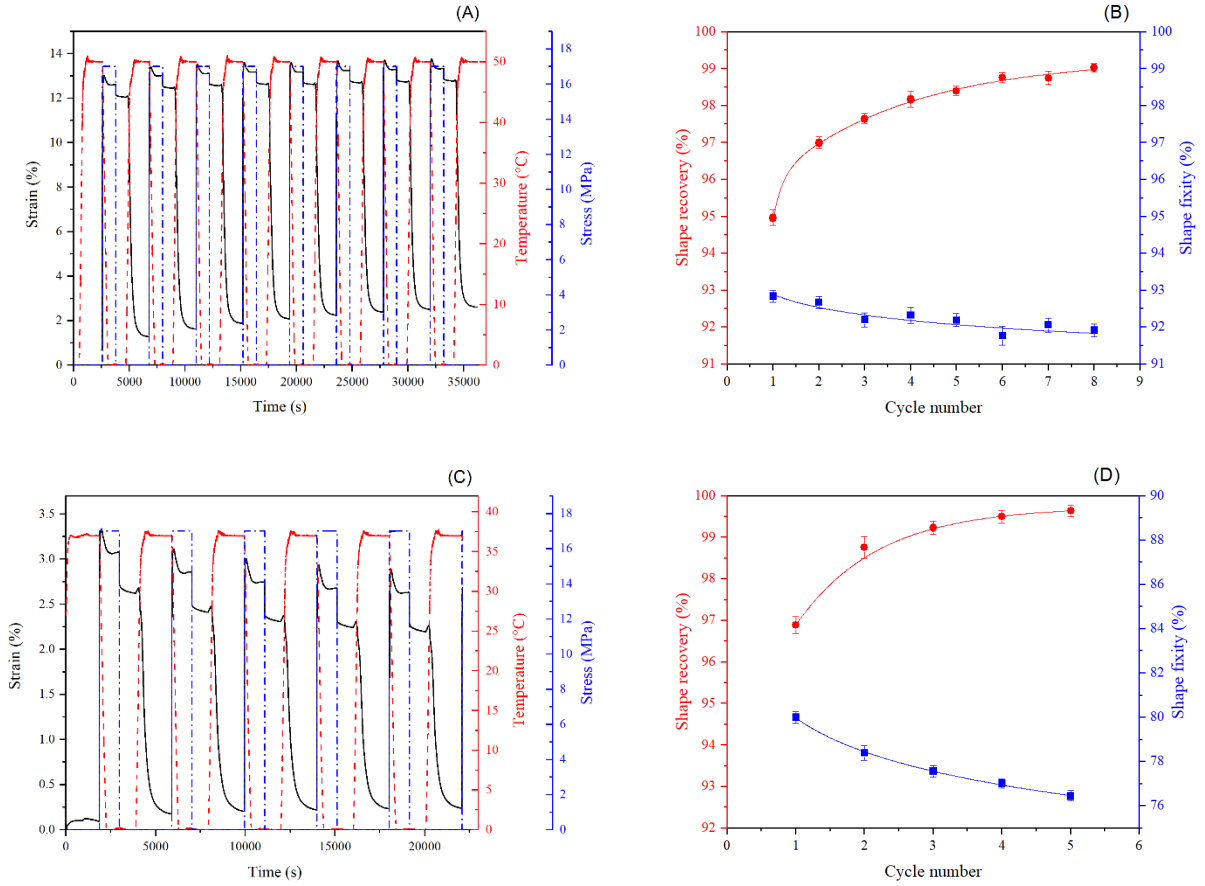

Figure 8. Representative shape memory cycles of PTF15PTSeb copolymer with 50 ºC (A) and 37 °C (C) as the deformation temperature; and shape fixation and shape recovery ratios of PTF15PTS copolymer for different cycles after deformation at 50 ºC (B) and 37 °C (D).

The consecutive cycling experiments indicate that the shape memory effect is highly reproducible, with recovery ratio over 95 % and fixation ratio over 91% throughout 8 cycles (Figure 8B). For each cycle, the recovery ratio increases from 94.9 %, reaching over 99 % in the last cycle. Conversely, the fixation rate, which has the highest value in the first cycle of 92.9%, decreases with each subsequent cycle. A similar dependency has been reported in the literature.[31][32][49]

The shape memory effect, with 37 °C as the deformation temperature was also investigated. The results are presented in Figure 8C and 8D. In this case, the shape fixity efficiency was over 76 % and shape recovery over 96 % throughout 6 cycles. When the stress was released after predeformation at low temperature, the polymer chains readily retract to their original shape to a great degree, leading to lower shape fixing ratio.

3.5. Gas barrier properties

Permeability tests to oxygen and carbon dioxide pure gases were carried out at 23 °C on the compression moulded films. The Gas Transmission Rate (GTR) values are shown in Table 5 and reported in Figure 9A. As known, gas passage through a polymer matrix is a complex phenomenon, being affected by many features, like T_g, T_m, crystallinity degree and perfection, and interactions between adjacent polymeric chain segments. In the particular case of furan-based polyesters, aromatic ring π-π stacking resulted particularly effective.[50][51][52] Besides these interactions, the additional establishment of side-by-side interchain C-H---O bonds occurs, possibly leading to the formation of a 2D ordered structure, defined as mesophase, different from the crystalline phase. Such phase has been already deeply investigated and unveiled.[1][53] The interchain physical connections are responsible for a very effective chain packing, hindering gas passage and thus giving to the material outstanding barrier properties, typical of those of liquid-crystalline polymers, which are one of the most performing classes among polymers. If the data collected in Table 5 and Figure 9A are considered, it can be noticed that all the materials are characterized by excellent barrier properties, comparable or even better than those of PET, and in line with those of PTF and other furan-based materials already studied.[1] More in details, PTF and PTF5PTSeb are characterized by low and comparable GTR values, being both in the glassy amorphous state at room temperature. As known, compared to the rubbery one, the glassy state is characterized by

lower chain mobility, which means minor free volume through which gases can pass. PTF15PTSeb copolymer is the most performing material, with GTR values to O_2 and CO_2 of 0.0022 and 0.0026 $cm^3 \cdot cm/m^2 \cdot d \cdot atm$, respectively. This outstanding result is particularly surprising, considering the polymer T_g is around room temperature and the sample is amorphous. These features, in conventional polymers, should determine high GTR values, since $T_g < T_{room}$ is responsible for a higher free volume and the crystalline phase, which makes gas path more difficult and tortuous through the polymeric matrix, is completely absent.

Table 5. GTR values (O_2, CO_2) of PTF and PTFcoPTSeb copolymers at 23 °C and 0 % RH, together with those of some PBAT copolymers and commercially available Ecoflex and EVOH EVAL.

Sample	O_2-TR (cm^3 cm / m^2 d atm)	CO_2-TR (cm^3 cm / m^2 d atm)
PTF	0.0800 ± 0.0100	0.0500 ± 0.0100
PTF5PTSeb	0.1295 ± 0.0200	0.1457 ± 0.0200
PTF15PTSeb	0.0022 ± 0.0010	0.0026 ± 0.0010
PTF25PTSeb	0.8212 ± 0.0200	2.3000 ± 0.1000
PTF* [1]	0.0224 ± 0.0050	0.0288 ± 0.0050
PBAT[a] [23]	6.630 ± 0.0657	79.40 ± 0.657
PBAT[b] [46]	10.2	111.0
Ecoflex[c] [35][54]	8.640 ± 0.196[c]	54.6[d]
EVOH EVAL™ [55]	0.0001- 0.0005	0.0001 - 0.0008

a – synthesized PBAT copolymer with 57 mol % of BA from ref. [23];
b – synthesized PBAT with 59 mol % of BA (Mw = 45 000 g/mol, PDI =1.6) measured at 30 °C, time lag permeation method;[46]
c - Ecoflex F-blend C1200 supplied by BASF (M_w= 53 900 g/mol, PDI=1.70), measured at 25 °C and 50 % RH;[36] d - CO_2-TR measured at 20 °C.[54]

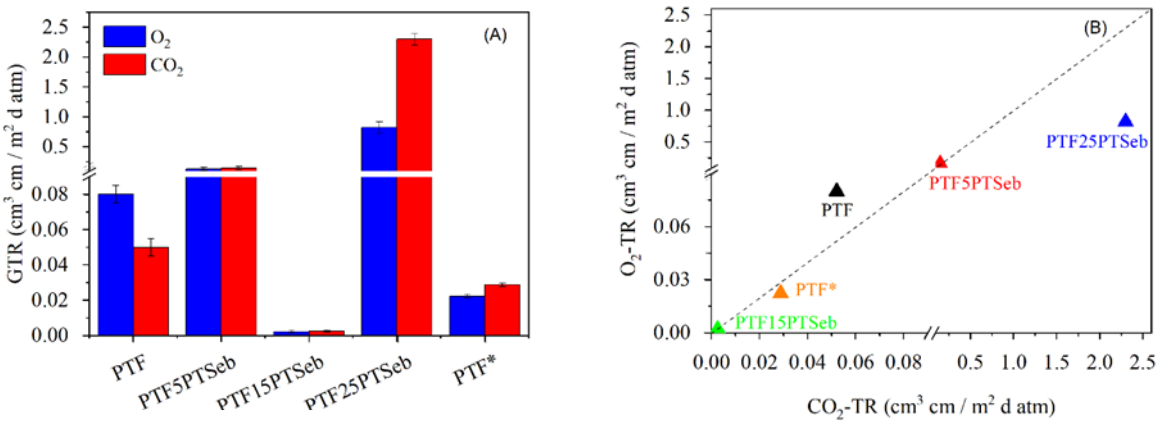

Figure 9. A) GTR values to O_2 and CO_2 and B) O_2-TR vs. CO_2-TR for PTF and PTFcoPTSeb copolymers, compared to those of PTF previously investigated (PTF*) (from ref. 1).

Again, this result can be explained as due to π-π stacking as well as of intermolecular interactions involving the ring hydrogen atoms and the carboxylic oxygen ones. It is possible that at room temperature, macromolecular chains are able to rearrange and interact, maximizing the interchain physical connections, making amorphous phase more compact, thus more effective in hampering gas passage. At the same time, the absence of crystals in the polymer matrix determines the reduction of interphase disclinations, these latter being possible preferential channels for the passage of gases. Lastly, PTF25PTSeb, which is semicrystalline with a T_g well below room temperature, is characterized by the highest values of GTR to both gases, probably due to the combination of the different factors mentioned above, i.e. a higher amount of disclinations between crystalline and amorphous domains and a greater free volume related to the lower T_g. In Figure 9B, the transmission rate values to oxygen (O_2-TR) are reported as a function of transmission rate values to carbon dioxide (CO_2-TR) for the polyesters under investigation and for a PTF film

previously studied (PTF*).[1] As known, perm-selectivity ratio, i.e. GTR-CO_2/GTR-O_2 value, indicates the different barrier performance towards the two gases that, in turn, depends on both gas diffusivity and solubility. In general, the GTR trend depends on several factors, among them, gas molecule diameter and affinity between permeating species and polymer matrix. Higher values of CO_2-TR are common for polymer films.[56] One can assume that the balance between these factors (size and affinity) determines higher permeability and thus greater GRT values for CO_2. However, as already investigated in previous works[1] on furan-based polyesters, this ratio is about 1, meaning the solubility of CO_2 is increased as a result of the presence of permanent dipoles in this gas molecule interacting with the polar groups of polymeric chains (ester groups as well as furan ring). In the materials under investigation, the GTR-CO_2/GTR-O_2 ratio is always close to 1, in agreement with other furan-based polyesters previously investigated, except for PTF25PTSeb. This result is not surprising, considering that the introduction of 25 mol % of TSeb non-polar co-unit is responsible for a lowering of the polar character of polymeric matrix, thus resulting in higher perm-selectivity ratio. From the comparison with the GTR data of fossil-based PBTA,[23] it can be evicted that all the samples under investigation are significantly more performant to both gases, the corresponding TR-O_2 and TR-CO_2 being from 1 to 3 order of magnitude and from 35 times to 4 order of magnitude lower, respectively. Also the values of Ecoflex are worse than those obtained from the materials under investigation, of at least one order of magnitude.[36][51] In addition, the PTF15PTSeb copolymer can compete with non-biodegradable ethylene-vinyl alcohol copolymer (EVOH) film, which offers outstanding barrier properties to O_2 and CO_2 (Table 6), although the performances highly depend on the RH of the environment.[39]

3.6. Composability of PTF and PTFcoPTSeb copolymers

To check the compostability of PTF and its copolymers, all the samples have been incubated in compost and withdrawn at different time points. Figure 10A shows the percentage gravimetric

weight loss after 1 up to 6 months of incubation. It is clear that the degradation rate is strictly related to the molar copolymer composition: in fact, for PTF and PTF5PTSeb, the weight loss is practically negligible (reaching values of just 2 and 5 % after 6 months, respectively). Conversely, in the case of the two copolymers richer in TSeb co-units, a completely different behavior can be observed. More in detail, PTF15PTSeb loses almost 80 % of its initial weight after 6 months, while PTF25PTSeb undergoes complete degradation after only 4 months of incubation.

Molecular weight loss measurements were also carried out, in order to better understand the nature of degradation process, taking into account that samples in compost are subjected to both enzymatic degradation on the surface and hydrolytic one in the bulk. The percentage molecular weight loss values of PTF and PTFcoTSEB copolymers at different timepoints are reported in Figure 10A. As it can be seen, incubation in compost is responsible for a decrease in molecular weight for all the materials under investigation, even for those, which did not show an appreciable gravimetric weight loss. Moreover, ^{1}H-NMR analysis carried out on degraded samples (data not shown) revealed that composition remains constant, in line with random distribution of the sequences. However, as to molecular weight loss data, they decrease as a function of time and TSeb co-unit amount, indicating that aliphatic sequences are those preferably attacked. More in details, PTF and PTF5PTSeb show an almost negligible variation of gravimetric weight, although a decrease of molecular weight after 6 months of incubation (of 30 % and 60 %), was observed. Conversely, copolymers richer in TSeb co-units undergo significant degradation over time, with a decrease of both gravimetric and molecular weight. Interestingly, PTF25PTSeb, although is the fastest degrading sample, in agreement with its composition, shows a reduced molecular weight loss with respect to PTF15PTSeb, as a consequence of its higher crystallinity.

The degradation process was also macroscopically evaluated by observing polymeric surfaces at different timepoints: as it can be seen from Figure 10C, even at shorter incubation times, all the samples turned opaque as a result of sample crystallization at composting temperature, which was comparable (PTF) or higher than their T_g (copolymers).

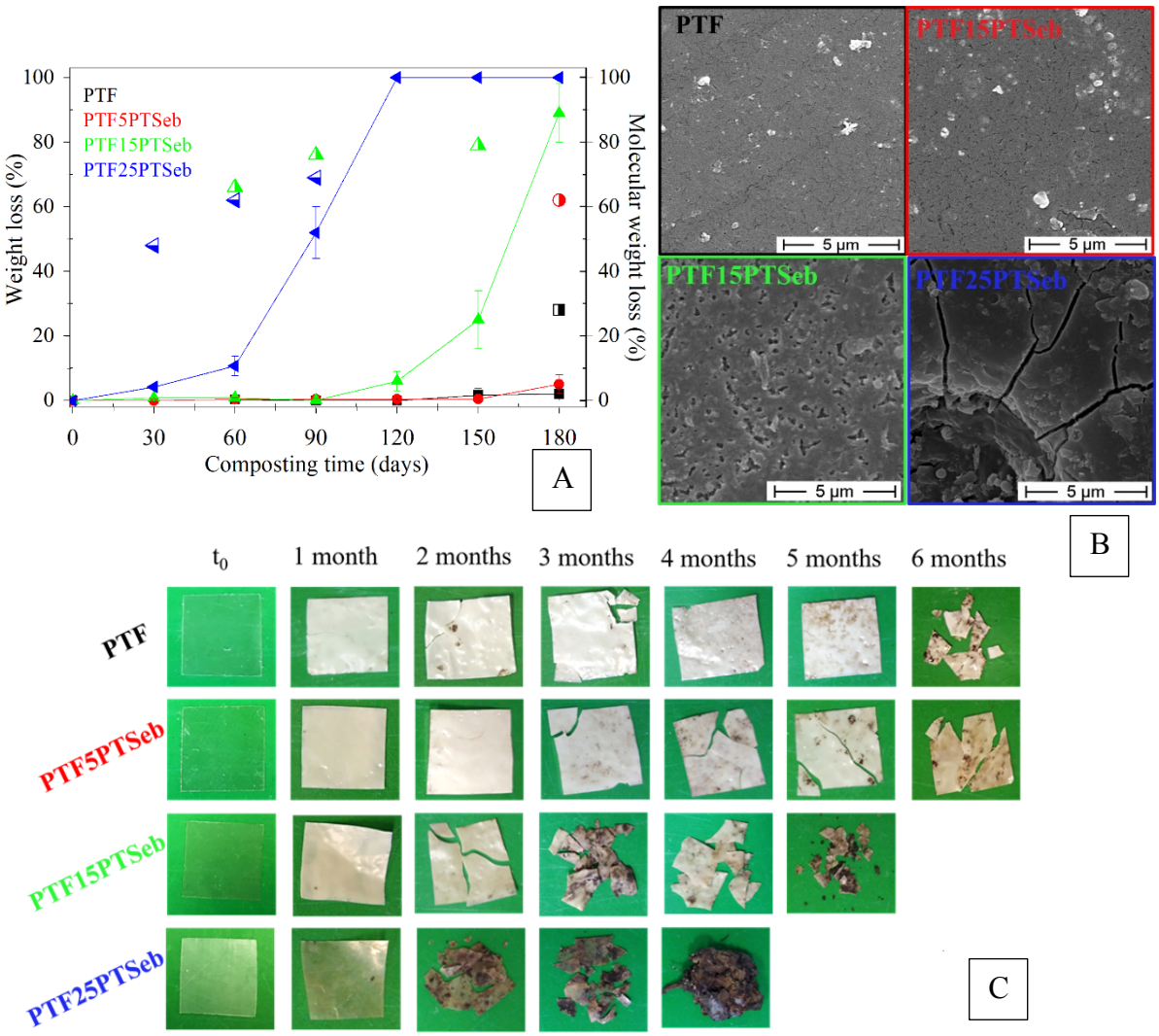

Figure 10. A) Percentage weight (filled symbols) and molecular weight loss (half-filled symbols) as a function of incubation time; B) SEM images of the partially degraded PTF, PTF5PTSeb (6 months of incubation), PTF15PTSeb (3 months of incubation) and PTF25PTSeb (2 months of incubation); C) Images of PTF and its copolymers recovered from compost at each incubation time.

In addition, the PTF homopolymer and the PTF5PTSeb copolymer undergo significant fragmentation after 6 and 4 months, respectively, suggesting the materials become more fragile and, although a negligible weight loss was measured, probably enzymes started the degradation process. Conversely, the two copolymers richer in PTSeb co-unit show significant fragmentation and turned darker even at shorter times. In particular, in the case of PTF25PTSeb recovered from the compost after 4 months, only a slight polymeric halo at the surface of the compost layer could be detected, meaning that a complete degradation occurred.

The effect of the incubation in compost has been also microscopically evaluated by means of scanning electron microscopy (SEM). This analysis was carried out in order to: i) check whether some degradation occurs at longer times (6 months) even in samples which do not undergo gravimetric weight loss; ii) follow the initial enzymatic attack (3 months for PTF15PTSeb and 2 months for PTF25PTSeb) for degradable samples. As it can be seen from Figure 10B, despite the very small weight loss, the surfaces of PTF and PTF5PTSeb films show some little holes/fractures, attesting that a minor degradation process affects these two samples too. In the case of PTF15PTSeb, as already suggested by the weight loss results, even after 3 months of incubation the enzymatic attack is evident, being the entire surface characterized by voids. The initial degradation is even more pronounced for PTF25PTSeb after 2 months of incubation, in this case deep fractures and holes being present on the polymeric surface.

The composting effect on the whole polymer matrix was evaluated by calorimetric measurements. The I scan DSC curves of partially degraded samples at different time points together with their blanks, annealed at 58 °C for 1 month (the longer time blanks did not further evolve) are reported Figure 11 and the relative thermal transitions data are listed in Table 3S.

If the DSC traces of the blank samples are compared to those of the neat films, some differences can be observed: in details, in PTF two melting phenomena (around 103 and 165 °C) appear, as a consequence of crystal development occurred during the permanence at the incubation temperature, close to T_g. As previously detailed in [38]-[40] the multiple melting behavior present in this sample could be due to polymorphism, which is characteristic for PTF crystallized at temperatures below 100 °C. In addition, the sharp jump around T_g due to chain shrinkage disappears.

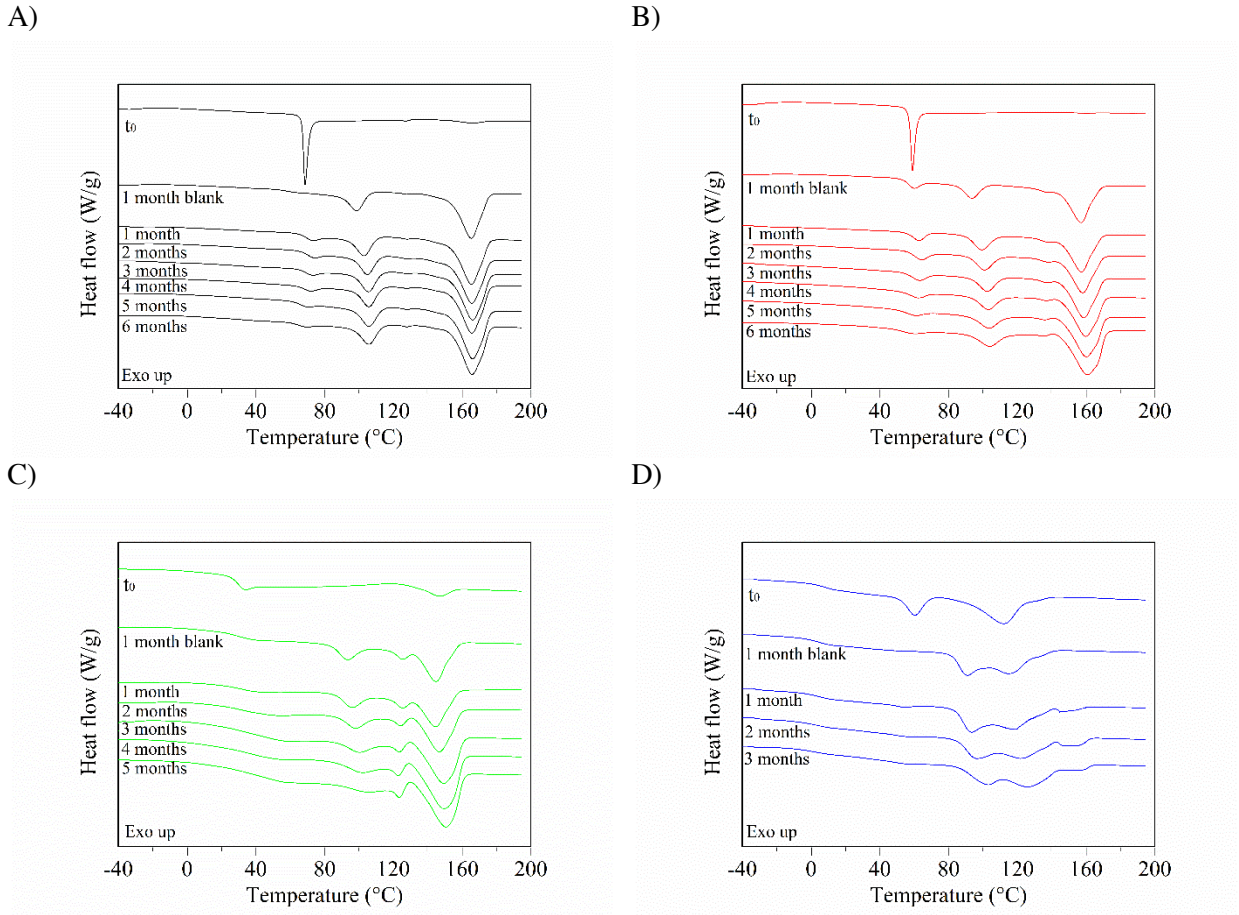

Figure 11. First heating DSC curves of partially degraded samples at different time points together with their blanks, annealed at 58 °C for 1 month: A) PTF; B) PTF5PTSeb; C) PTF15PTSeb; D) PTF25PTSeb.

Blank PTF5PTSeb shows a behavior similar to PTF, as also in this case multiple melting phenomena are present, together with the disappearance of the jump just above T_g, related to chain constrictions. As to PTF15PTSeb, three endothermic phenomena around 100, 125 and 150 ºC arose, again as a result of the permanence at 58 °C, while for the already semicrystalline PTF25PTSeb film, only a shift of the melting peak initially at 60 ºC to about 90 °C, was detected. Also for the copolymers, the multiple melting phenomena could be associated to the polymorphism of PTF.

As to partially degraded samples, for PTF, a progressive decrease in T_g and ΔC_p values can be observed. The T_g decrease can be ascribed to the presence of water incorporated into the macromolecular chains, acting as plasticizer, while the lower ΔC_p values can be related to the reduction of amorphous phase converted into crystals, as evidenced by the appearance of endothermic peaks at higher temperature. In addition, the sharp jump around T_g is still absent, as a consequence of relaxation occurring during incubation at 58 ºC. As to the multiple melting phenomena already observed in the blank specimen, they remain almost unvaried both in position and in intensity, only an increase of the highest temperature endotherm asymmetry, with respect to the blank traces, can be detected. This latter can indicate the formation of a crystalline phase with high perfection, resulting from hydrolyzed PTF chains capable to crystallize into the most perfect crystalline phase.

A similar trend was observed for PTF5PTSeb in terms of glass-to-rubber transition and melting phenomena, being in this case the highest melting peak shifted to lower temperature with respect to PTF, due to the presence of TSeb co-unit, as already observed for the neat film.

For PTF15PTSeb, apart from the presence of the multiple endothermic phenomena evicted also in the blank sample, the effect of enzymatic attack regarded mainly the amorphous and the less-

perfect crystalline phase and induced a decrease of both T_g and ΔC_p values, together with a progressive flattening of the lowest melting peak. Again, the increasing of the highest melting peak asymmetry was evidenced. This result can be explained by progressive preferential enzyme attack towards TSeb segments leading to the formation of pure PTF chain fragments, which can undergo crystallization. Lastly, by observing DSC traces of PTF25PTSeb, a progressive improvement of crystalline phase was observed during the degradation process. As already noticed for PTF15PTSeb, the decrease of T_g and ΔC_p, the progressive flattening of the lowest melting peak as well as the increase of ΔH_m of the peak at highest temperature con be considered proof of the preferential enzymatic attack of amorphous and less perfect crystalline regions. Finally, in PTF25PTSeb DSC curves after 1, 2 and 3 months of composting, a shoulder, around 150 ºC, which increased in intensity with time, can be observed. A possible explanation of what observed can be found again in the formation of short PTF homopolymer chains, which remain after degradation of TSeb moieties, capable of crystallizing into pure high-melting PTF crystalline lattice.

The presented results of compostability indicated that PTFcoPTSeb copolymer containing 25 mol % of TSeb will be able to fulfill the requirements of the EN 13432 and ASTM D6400 standards used for evaluating biodegradability of plastics, which requires 90% weight loss in less than 6 months.[28][57] The evaluation criteria including material characteristics, biodegradation, disintegration and compost quality, which are outlined in these standards needs to be filled for each compostable material.[58],[59] The compostability of PTF25PTSeb is comparable to Ecofex containing higher content of aliphatic comonomeric unit (about 50 mole % of BA) which is compostable within 6 months.

4. Conclusions

Novel high molecular weight 100% bio-based random aliphatic-aromatic copolymers of PTF containing different amounts of sebacic acid were successfully synthesized by eco-friendly polycondensation in the melt. The all used co-monomers were derived from fast-renewable resources, such as castor oil and sugars. Copolymerization of PTF has proved to be a winning strategy to:

i) reduce its rigidity and fragility,

ii) improve its gas barrier properties to both oxygen and carbon dioxide,

iii) increase its rate of biodegradation under composting conditions,

iv) finely tune polymer final property acting on copolymer composition.

Specifically, the T_g of copolymers decreased from 48 to 10 ºC, for PTSeb co-unit content ranging from 5 to 25 mol %.

PTF and copolyesters containing 5 and 15 mol % of PTSEb, were amorphous polymers at room temperature, whereas the copolyester containing 25 mol % of PTSeb, developed a crystalline phase during storage at room temperature. The Young modulus of copolyesters ranged from 2500 to 289 MPa, the tensile strength decreased from 77 to 17 MPa, while the elongation at break increased from 3 to 410 %. Additionally, the copolyester with 15 mol % of PTSeb exhibited temperature induced shape memory behavior, which foreshadows possible new applications, including as example biomedical ones, for these new PTF copolymers beyond food packaging ones.

All the polymers under investigation are characterized by outstanding gas barrier properties to both gases, PTF15PTSeb copolymer being however by far the best performing material, with GTR values to O_2 and CO_2 of 0.0022 and 0.0026 $cm^3 \cdot cm/m^2 \cdot d \cdot atm$, respectively. These values are 35 and

20 times lower than those of PTF and comparable to those of EVOH, currently used in multilayer packaging films to ensure high barrier.

Copolyesters containing 15 and 25 mol % of PTSeb co-units are compostable, the first one loses around 90 % of its initial weight after 6 months, the latter one undergoes complete degradation after only 4 months of incubation.

In summary, low amounts of PTSeb comonomeric units significantly modify PTF thermal, mechanical and barrier properties and render the final material compostable. PTF15PTSeb resulted the sample with properties similar to those of commercially available compostable Ecoflex® polymer, but with markedly improved barrier properties.[55]

Supporting Information

"Supporting information: Additional_info_PTFcoPTSeb.PDF

Author Contributions

A.Z. copolymers synthesis and characterization, investigations of thermal, tensile properties and SMP. A.S. conceptualization and supervision of the research activity, validation, writing original draft. R.S. SEC measurements. G.G. composting experiments; correction and revision of the manuscript. M.S supervision of experimental activity; analysis of the overall experimental data; correction and revision of the manuscript. V.S. gas barrier measurements and corresponding data analysis; correction and revision of the manuscript. N.L. supervision of experimental activity; analysis of the overall experimental data; correction and revision of the manuscript; supervision of the work and research funding.

The authors declare no conflicts of interest.

ACKNOWLEDGMENT

This publication is based upon work from COST Action FUR4Sustain, CA18220, supported by COST (European Cooperation in Science and Technology). The authors thank Dr. Massimo Gazzano for his cooperation in the acquisition of SEM micrographs.

REFERENCES

[1] G. Guidotti, M. Soccio, M.C. García-Gutiérrez, T. Ezquerra, V. Siracusa, E. Gutiérrez-Fernández, A. Munari, N. Lotti, Fully Biobased Superpolymers of 2,5-Furandicarboxylic Acid with Different Functional Properties: From Rigid to Flexible, High Performant Packaging Materials, ACS Sustainable Chemistry & Engineering. 8 (2020) 9558–9568. https://doi.org/10.1021/ACSSUSCHEMENG.0C02840.

[2] J. Zhang, Y. Liu, Z. Qi, L. He, L. Peng, Progress in the synthesis and properties of 2,5-furan dicarboxylate based polyesters, BioResources. 15 (2020) 4502–4527. https://doi.org/10.15376/biores.15.2.4502-4527.

[3] X. Fei, X. Fei, X. Fei, J. Wang, J. Wang, J. Zhu, J. Zhu, X. Wang, X. Liu, X. Liu, Biobased Poly(ethylene 2,5-furancoate): No Longer an Alternative, but an Irreplaceable Polyester in the Polymer Industry, ACS Sustainable Chemistry and Engineering. 8 (2020) 8471–8485. https://doi.org/10.1021/acssuschemeng.0c01862.

[4] G. Guidotti, M. Soccio, N. Lotti, M. Gazzano, V. Siracusa, A. Munari, Poly(propylene 2,5-thiophenedicarboxylate) vs. Poly(propylene 2,5-furandicarboxylate): Two examples of high gas barrier bio-based polyesters, Polymers. 10 (2018) 785. https://doi.org/10.3390/polym10070785.

[5] L. Genovese, N. Lotti, V. Siracusa, A. Munari, Poly(neopentyl glycol furanoate): A member of the furan-based polyester family with smart barrier performances for sustainable food packaging applications, Materials. 10 (2017) 1028. https://doi.org/10.3390/ma10091028.

[6] A. Zubkiewicz, S. Paszkiewicz, A. Szymczyk, The effect of annealing on tensile properties of injection molded biopolyesters based on 2,5-furandicarboxylic acid, Polymer Engineering and Science. 61 (2021) 1536–1545. https://doi.org/10.1002/pen.25675.

[7] K. Loos, R. Zhang, I. Pereira, B. Agostinho, H. Hu, D. Maniar, N. Sbirrazzuoli, A.J.D. Silvestre, N. Guigo, A.F. Sousa, A Perspective on PEF Synthesis, Properties, and End-Life, Frontiers in Chemistry. 8 (2020) 585. https://doi.org/10.3389/fchem.2020.00585.

[8] M. Vannini, P. Marchese, A. Celli, C. Lorenzetti, Fully biobased poly(propylene 2,5-furandicarboxylate) for packaging applications: excellent barrier properties as a function of crystallinity, Green Chemistry. 17 (2015) 4162–4166. https://doi.org/10.1039/c5gc00991j.

[9] A. Tullo, DuPont, ADM Eye Biobased Polyester, C&EN Global Enterprise. 94 (2016) 6–6. https://doi.org/10.1021/cen-09404-notw2.

[10] F. Acquasanta, R. Visser, B. Langius, PEF as a multilayer barrier technology : a sustainable way to enable long shelf life in PET bottles, ComPETence Magazine. 2 (2020) 56–61. https://doi.org/10.1021/ma5000199/2/ComPETence.

[11] W. Takarada, K. Sugimoto, H. Nakajima, H.A. Visser, G.J.M. Gruter, T. Kikutani, Melt-spun fibers from bio-based polyester–fiber structure development in high-speed melt spinning of poly(ethylene 2,5-furan dicarboxylate) (PEF), Materials. 14 (2021) 1–14. https://doi.org/10.3390/ma14051172.

[12] S. Chen, R. Zou, L. Li, J. Shang, S. Lin, J. Lan, Preparation of biobased poly(propylene 2,5-furandicarboxylate) fibers: Mechanical, thermal and hydrolytic degradation properties, Journal of Applied Polymer Science. 138 (2021) app50345. https://doi.org/10.1002/app.50345.

[13] M. Soccio, N. Lotti, A. Munari, E. Rebollar, D.E. Martínez-Tong, Wrinkling poly(trimethylene 2,5-furanoate) free-standing films: Nanostructure formation and physical properties, Polymer. 202 (2020) 122666. https://doi.org/10.1016/j.polymer.2020.122666.

[14] M. Kwiatkowska, I. Kowalczyk, K. Kwiatkowski, A. Szymczyk, Z. Rosłaniec, Fully biobased multiblock copolymers of furan-aromatic polyester and dimerized fatty acid: Synthesis and characterization, Polymer. 99 (2016) 503–512. https://doi.org/10.1016/j.polymer.2016.07.060.

[15] M. Kwiatkowska, I. Kowalczyk, A. Szymczyk, K. Goracy, Effect of thermal aging on the crystalline structure and mechanical performance of fully bio-based, furan-ester, multiblock copolymers, Polimery. 63 (2018) 594–602. https://doi.org/10.14314/polimery.2018.9.3.

[16] H. Hu, R. Zhang, J. Wang, W. Bin Ying, J. Zhu, Fully bio-based poly(propylene succinate-co-propylene furandicarboxylate) copolyesters with proper mechanical, degradation and barrier properties for green packaging applications, European Polymer Journal. 102 (2018) 101–110. https://doi.org/10.1016/j.eurpolymj.2018.03.009.

[17] Z. Terzopoulou, L. Papadopoulos, A. Zamboulis, D.G. Papageorgiou, G.Z. Papageorgiou, D.N. Bikiaris, Tuning the properties of furandicarboxylic acid-based polyesters with copolymerization: A review, Polymers. 12 (2020). https://doi.org/10.3390/POLYM12061209.

[18] G. Guidotti, L. Genovese, M. Soccio, M. Gigli, A. Munari, V. Siracusa, N. Lotti, Block copolyesters containing 2,5-furan and trans-1,4-cyclohexane subunits with outstanding gas barrier properties, International Journal of Molecular Sciences. 20 (2019) 2187. https://doi.org/10.3390/ijms20092187.

[19] D. Perin, D. Rigotti, G. Fredi, G.Z. Papageorgiou, D.N. Bikiaris, A. Dorigato, Innovative Bio-based Poly(Lactic Acid)/Poly(Alkylene Furanoate)s Fiber Blends for Sustainable Textile Applications, Journal of Polymers and the Environment. (2021) 1–16. https://doi.org/10.1007/s10924-021-02161-y.

[20] N. Poulopoulou, G. Kantoutsis, D.N. Bikiaris, D.S. Achilias, M. Kapnisti, G.Z. Papageorgiou, Biobased engineering thermoplastics: Poly(butylene 2,5-furandicarboxylate) blends, Polymers. 11 (2019) 937. https://doi.org/10.3390/polym11060937.

[21] N. Poulopoulou, N. Kasmi, M. Siampani, Z.N. Terzopoulou, D.N. Bikiaris, D.S. Achilias, D.G. Papageorgiou, G.Z. Papageorgiou, Exploring next-generation engineering bioplastics: Poly(alkylene furanoate)/poly(alkylene terephthalate) (PAF/PAT) blends, Polymers. 11 (2019). https://doi.org/10.3390/polym11030556.

[22] G. Wang, M. Jiang, Q. Zhang, R. Wang, G. Zhou, Biobased copolyesters: synthesis, crystallization behavior, thermal and mechanical properties of poly(ethylene glycol sebacate-co-ethylene glycol 2,5-furan dicarboxylate), RSC Advances. 7 (2017) 13798–13807. https://doi.org/10.1039/c6ra27795k.

[23] F. Huang, L. Wu, B.G. Li, Sulfonated biodegradable PBAT copolyesters with improved gas barrier properties and excellent water dispersibility: From synthesis to structure-property, Polymer Degradation and Stability. 182 (2020) 109391. https://doi.org/10.1016/j.polymdegradstab.2020.109391.

[24] S. RameshKumar, P. Shaiju, K.E. O'Connor, R.B. P, Bio-based and biodegradable polymers - State-of-the-art, challenges and emerging trends, Current Opinion in Green and Sustainable Chemistry. 21 (2020) 75–81. https://doi.org/10.1016/j.cogsc.2019.12.005.

[25] H. Hu, R. Zhang, J. Wang, W. Bin Ying, L. Shi, C. Yao, Z. Kong, K. Wang, J. Zhu, A mild method to prepare high molecular weight poly(butylene furandicarboxylate-co-glycolate) copolyesters: Effects of the glycolate content on thermal, mechanical, and barrier properties and biodegradability, Green Chemistry. 21 (2019) 3013–3022. https://doi.org/10.1039/c9gc00668k.

[26] M. Soccio, M. Costa, N. Lotti, M. Gazzano, V. Siracusa, E. Salatelli, P. Manaresi, A. Munari, Novel fully biobased poly(butylene 2,5-furanoate/diglycolate) copolymers containing ether linkages: Structure-property relationships, European Polymer Journal. 81 (2016) 397–412. https://doi.org/10.1016/j.eurpolymj.2016.06.022.

[27] S. Peng, B.S. Wu, L. Wu, B.G. Li, P. Dubois, Hydrolytic degradation of biobased poly(butylene succinate-co-furandicarboxylate) and poly(butylene adipate-co-furandicarboxylate) copolyesters under mild conditions, Journal of Applied Polymer Science. 134 (2017) 44674. https://doi.org/10.1002/app.44674.

[28] S. Peng, L. Wu, B.G. Li, P. Dubois, Hydrolytic and compost degradation of biobased PBSF and PBAF copolyesters with 40–60 mol% BF unit, Polymer Degradation and Stability. 146 (2017) 223–228. https://doi.org/10.1016/j.polymdegradstab.2017.07.016.

[29] G.Z. Papageorgiou, D.G. Papageorgiou, V. Tsanaktsis, D.N. Bikiaris, Synthesis of the bio-based polyester poly(propylene 2,5-furan dicarboxylate). Comparison of thermal behavior and solid state structure with its terephthalate and naphthalate homologues, Polymer. 62 (2015) 28–38. https://doi.org/10.1016/j.polymer.2015.01.080.

[30] G.Z. Papageorgiou, D.S. Achilias, D.N. Bikiaris, Crystallization kinetics and melting behaviour of the novel biodegradable polyesters poly(propylene azelate) and poly(propylene sebacate), Macromolecular Chemistry and Physics. 210 (2009) 90–107. https://doi.org/10.1002/macp.200800441.

[31] I. Irska, S. Paszkiewicz, K. Gorący, A. Linares, T.A. Ezquerra, R. Jędrzejewski, Z. Rosłaniec, E. Piesowicz, Poly(Butylene terephthalate)/polylactic acid based copolyesters and blends: Miscibility-structure-property relationship, Express Polymer Letters. 14 (2020) 26–47. https://doi.org/10.3144/expresspolymlett.2020.4.

[32] X. Xiao, D. Kong, X. Qiu, W. Zhang, Y. Liu, S. Zhang, F. Zhang, Y. Hu, J. Leng, Shape memory polymers with high and low temperature resistant properties, Scientific Reports. 5 (2015) 1–12. https://doi.org/10.1038/srep14137.

[33] D. Maniar, Y. Jiang, A.J.J. Woortman, J. van Dijken, K. Loos, Furan-Based Copolyesters from Renewable Resources: Enzymatic Synthesis and Properties, ChemSusChem. 12 (2019) 990–999. https://doi.org/10.1002/cssc.201802867.

[34] H. Kim, T. Kim, S. Choi, H. Jeon, D.X. Oh, J. Park, Y. Eom, S.Y. Hwang, J.M. Koo, Remarkable elasticity and enzymatic degradation of bio-based poly(butylene adipate-co-furanoate): replacing terephthalate, Green Chemistry. 22 (2020) 7778–7787. https://doi.org/10.1039/D0GC01688H.

[35] A.R. de Matos Costa, A. Crocitti, L.H. de Carvalho, S.C. Carroccio, P. Cerruti, G. Santagata, Properties of biodegradable films based on poly(Butylene succinate) (pbs) and poly(butylene adipate-co-terephthalate) (pbat) blends, Polymers. 12 (2020) 1–17. https://doi.org/10.3390/polym12102317.

[36] H. Kargarzadeh, A. Galeski, A. Pawlak, PBAT green composites: Effects of kraft lignin particles on the morphological, thermal, crystalline, macro and micromechanical properties, Polymer. 203 (2020) 122748. https://doi.org/10.1016/J.POLYMER.2020.122748.

[37] F. Chivrac, Z. Kadlecová, E. Pollet, L. Avérous, Aromatic copolyester-based nano-biocomposites: Elaboration, structural characterization and properties, Journal of Polymers and the Environment. 14 (2006) 393–401. https://doi.org/10.1007/s10924-006-0033-4.

[38] M.C. Righetti, P. Marchese, M. Vannini, A. Celli, F. Tricoli, C. Lorenzetti, Temperature-induced polymorphism in bio-based poly(propylene 2,5-furandicarboxylate), Thermochimica Acta. 677 (2019) 186–193. https://doi.org/10.1016/j.tca.2018.12.003.

[39] L. Genovese, M. Soccio, N. Lotti, A. Munari, A. Szymczyk, S. Paszkiewicz, A. Linares, A. Nogales, T.A. Ezquerra, Effect of chemical structure on the subglass relaxation dynamics of biobased polyesters as revealed by dielectric spectroscopy: 2,5-furandicarboxylic acid vs. trans-1,4-cyclohexanedicarboxylic acid, Physical Chemistry Chemical Physics. 20 (2018) 15696–15706. https://doi.org/10.1039/C8CP01810C.

[40] M.C. Righetti, P. Marchese, M. Vannini, A. Celli, C. Lorenzetti, D. Cavallo, C. Ocando, A.J. Müller, R. Androsch, Polymorphism and Multiple Melting Behavior of Bio-Based

Poly(propylene 2,5-furandicarboxylate), Biomacromolecules. 21 (2020) 2622–2634. https://doi.org/10.1021/acs.biomac.0c00039.

[41] N. Lotti, M. Soccio, M. Gazzano, L. Finelli, A. Munari, Copolymerization: A new tool to selectively induce poly(butylene naphthalate) crystal form, Journal of Polymer Science, Part B: Polymer Physics. 47 (2009) 1356–1367. https://doi.org/10.1002/polb.21740.

[42] J. Jian, Z. Xiangbin, H. Xianbo, An overview on synthesis, properties and applications of poly(butylene-adipate-co-terephthalate)–PBAT, Advanced Industrial and Engineering Polymer Research. 3 (2020) 19–26. https://doi.org/10.1016/j.aiepr.2020.01.001.

[43] K. Fukushima, M.H. Wu, S. Bocchini, A. Rasyida, M.C. Yang, PBAT based nanocomposites for medical and industrial applications, Materials Science and Engineering: C. 32 (2012) 1331–1351. https://doi.org/10.1016/J.MSEC.2012.04.005.

[44] K. Chrissafis, K.M. Paraskevopoulos, G.Z. Papageorgiou, D.N. Bikiaris, Thermal decomposition of poly(propylene sebacate) and poly(propylene azelate) biodegradable polyesters: Evaluation of mechanisms using TGA, FTIR and GC/MS, Journal of Analytical and Applied Pyrolysis. 92 (2011) 123–130. https://doi.org/10.1016/j.jaap.2011.05.001.

[45] V. Tsanaktsis, E. Vouvoudi, G.Z. Papageorgiou, D.G. Papageorgiou, K. Chrissafis, D.N. Bikiaris, Thermal degradation kinetics and decomposition mechanism of polyesters based on 2,5-furandicarboxylic acid and low molecular weight aliphatic diols, Journal of Analytical and Applied Pyrolysis. 112 (2015) 369–378. https://doi.org/10.1016/J.JAAP.2014.12.016.

[46] H. Beneš, J. Kredatusová, J. Peter, S. Livi, S. Bujok, E. Pavlova, J. Hodan, S. Abbrent, M. Konefał, P. Ecorchard, Ionic Liquids as Delaminating Agents of Layered Double Hydroxide during In-Situ Synthesis of Poly (Butylene Adipate-co-Terephthalate) Nanocomposites, Nanomaterials 2019, Vol. 9, Page 618. 9 (2019) 618. https://doi.org/10.3390/NANO9040618.

[47] Z. Gan, K. Kuwabara, M. Yamamoto, H. Abe, Y. Doi, Solid-state structures and thermal properties of aliphatic–aromatic poly(butylene adipate-co-butylene terephthalate) copolyesters, Polymer Degradation and Stability. 83 (2004) 289–300. https://doi.org/10.1016/S0141-3910(03)00274-X.

[48] T.D. Nguyen, Modeling shape-memory behavior of polymers, Polymer Reviews. 53 (2013) 130–152. https://doi.org/10.1080/15583724.2012.751922.

[49] C. Li, X. Ji, Y. Tu, Y. Zheng, J. Shen, S. Guo, Self-Optimization of the Shape-Memory Effect during Programming Cycle Tests, Macromolecules. 54 (2021) 214–224. https://doi.org/10.1021/acs.macromol.0c01961.

[50] T. Sago, H. Itagaki, T. Asano, Onset of forming ordering in uniaxially stretched poly(ethylene terephthalate) films due to π-π Interaction clarified by the fluorescence technique, Macromolecules. 47 (2014) 217–226. https://doi.org/10.1021/ma401806u.

[51] T.P. Kaloni, P.K. Giesbrecht, G. Schreckenbach, M.S. Freund, Polythiophene: From Fundamental Perspectives to Applications, Chemistry of Materials. 29 (2017) 10248–10283. https://doi.org/10.1021/acs.chemmater.7b03035.

[52] V.Y. Rudyak, A.A. Gavrilov, D. V. Guseva, S.H. Tung, P. V. Komarov, Accounting for π-π Stacking interactions in the mesoscopic models of conjugated polymers, Molecular Systems Design and Engineering. 5 (2020) 1137–1146. https://doi.org/10.1039/d0me00034e.

[53] G. Guidotti, M. Soccio, M.C. García-Gutiérrez, E. Gutiérrez-Fernández, T.A. Ezquerra, V. Siracusa, A. Munari, N. Lotti, Evidence of a 2D-Ordered Structure in Biobased Poly(pentamethylene furanoate) Responsible for Its Outstanding Barrier and Mechanical Properties, ACS Sustainable Chemistry and Engineering. 7 (2019) 17863–17871. https://doi.org/10.1021/acssuschemeng.9b04407.

[54] S. Livi, G. Sar, V. Bugatti, E. Espuche, J. Duchet-Rumeau, Synthesis and physical properties of new layered silicates based on ionic liquids: improvement of thermal stability, mechanical behaviour and water permeability of PBAT nanocomposites, RSC Advances. 4 (2014) 26452–26461. https://doi.org/10.1039/C4RA02143F.

[55] L.W. McKeen, Polyolefins, Polyvinyls, and Acrylics, in: Permeability Properties of Plastics and Elastomers, Elsevier, 2012: pp. 145–193. https://doi.org/10.1016/b978-1-4377-3469-0.10009-8.

[56] G.L. Robertson, Optical, Mechanical and Barrier Properties of Thermoplastic Polymers, in: Food Packaging, CRC Press, Boca Raton, FL, USA, 2013: pp. 91-130. https://doi.org/10.1201/b21347-9.

[57] A. Künkel, J. Becker, L. Börger, J. Hamprecht, S. Koltzenburg, R. Loos, M.B. Schick, K. Schlegel, C. Sinkel, G. Skupin, M. Yamamoto, Polymers, Biodegradable, in: Ullmann's Encyclopedia of Industrial Chemistry, American Cancer Society, 2016: pp. 1–29. https://doi.org/10.1002/14356007.n21_n01.pub2.

[58] U. Witt, T. Einig, M. Yamamoto, I. Kleeberg, W.D. Deckwer, R.J. Müller, Biodegradation of aliphatic-aromatic copolyesters: Evaluation of the final biodegradability and ecotoxicological impact of degradation intermediates, Chemosphere. 44 (2001) 289–299. https://doi.org/10.1016/S0045-6535(00)00162-4.

[59] G. Kale, T. Kijchavengkul, R. Auras, M. Rubino, S.E. Selke, S.P. Singh, Compostability of bioplastic packaging materials: An overview, Macromolecular Bioscience. 7 (2007) 255–277. https://doi.org/10.1002/mabi.200600168.

Figures

Figure 1. Chemical structure of PTFcoPTSeb copolymers.

Figure 2. FTIR spectra of PTF and PTF-PTSeb random copolymers.

Figure 3. ^{1}H-NMR spectra of PTSeb, PTF25PTSeb in $CDCl_3$ and PTF, PTF5PTSeb, PTF15PTSeb in $CDCl_3/CF_3COOD$ 10:1 with relative peak assignment.

Figure 4. DSC heating and cooling scans at rate of 10, 5 and 3 ºC min-1 for PTF (a) and PTFcoPTSeb copolymers (b-d). For all samples, the first heating scan measured at 10 °C min-1 after 2 month storage at room temperature are reported (green curves).

Figure 5. Comparative XRD patterns for PTF and PTFcoPTSeb copolymers before and after annealing.

Figure 6. Stress-strain curves for PTF and PTFcoPTSeb copolymers before and after annealing (a) magnification of the region corresponding to small strain range (0-20%) (b).

Figure 7. Demonstration of shape recovery of dumbbell shape sample of PTF15PTSeb copolymer.

Figure 8. Shape memory cycles of PTF15PTSeb copolymer with 50 ºC (A) and 37 °C (B) as the deformation temperature; and shape fixation and shape recovery ratios of PTF15PTS copolymer for different cycles after deformation at 50 ºC (C) and 37 °C (D).

Figure 9. A) GTR values to O_2 and CO_2 and B) O_2-TR vs. CO_2-TR for PTF and PTFcoPTSeb copolymers, compared to those of PTF previously investigated (PTF*) (from ref. 1).

Figure 10. A) Percentage weight (filled symbols) and molecular weight loss (half-filled symbols) as a function of incubation time; B) SEM images of the partially degraded PTF, PTF5PTSeb (6

months of incubation), PTF15PTSeb (3 months of incubation) and PTF25PTSeb (2 months of incubation); C) Images of PTF and its copolymers recovered from compost at each incubation time.

Figure 11. I scan DSC curves of partially degraded samples at different time points together with their blanks, annealed at 58 ºC for 1 month: A) PTF; B) PTF5PTSeb; C) PTF15PTSeb; D) PTF25PTSeb.

Tables

Table 1. Composition, sequence length, degree of randomness and molecular weight of the PTFcoPTSeb copolymers.

Table 2. DSC data from first scans at 10 oC min-1 for PTF and PTFcoPTSeb copolymers, together with those of some PBAT copolymers and Ecoflex.

Table 3. TGA data for PTF and PTFcoPTSeb copolymers in air and argon atmosphere.

Table 4. Tensile properties of PTF and PTFcoPTSeb copolymers before and after annealing, together with those of some PBAT copolymers and Ecoflex.

Table 5. GTR values (O_2, CO_2) of PTF and PTFcoPTSeb copolymers at 23 °C and 0 % RH, together with those of some PBAT copolymers and commercially available Ecoflex and EVOH EVAL.